CONDUCTED SUPRA-HARMONIC EMISSIONS IN POWER DRIVE SYSTEMS

Lappeenranta–Lahti University of Technology LUT

Master’s Programme in Electrical Engineering, Master's thesis

2023

Jukka Salonen

Examiners: Professor Pasi Peltoniemi, D.Sc. (Tech.)

Ville Forsström, M.Sc. (Tech.)

ABSTRACT

Lappeenranta–Lahti University of Technology LUT

LUT School of Energy Systems

Electrical Engineering

Jukka Salonen

Conducted Supra-Harmonic Emissions in Power Drive Systems

Master’s thesis

2023

80 pages, 60 figures and 3 appendices

Examiners: Professor Pasi Peltoniemi, D.Sc. (Tech.) and Ville Forsström, M.Sc. (Tech.)

Keywords: Supra-harmonics, variable speed drive

Supra-harmonics have emerged as a new challenge for variable speed drive (VSD) manufacturers, as these will be addressed in forthcoming standards in the coming years. The IEC (SC77A WG1) is currently developing the upcoming IEC 61000-3-10 standard, which aims to define the maximum allowable values for voltage and current harmonics in the 2-9 kHz frequency range for electrical equipment with a rated current of up to 75 A.

This Master's thesis provides an overview of the standard by examining the draft document prepared by the IEC working group. Laboratory experiments were carried out to measure the conducted supra-harmonic emissions (2-9 kHz) of four different VSDs at various operating points. Based on the measurement results, the voltage and current emissions of these VSDs remain below the maximum limits specified in the standard draft. The practical suitability of the available measuring instruments was also investigated. Based on the findings, the measuring instruments are capable of analyzing the supra-harmonic emissions of the drives. Due to the absence of the new grouping method specified in the standard, the instruments, however, cannot yet perform official compliance measurements.

TIIVISTELMÄ

Lappeenrannan–Lahden teknillinen yliopisto LUT

LUT Energiajärjestelmät

Sähkötekniikka

Jukka Salonen

Johtuvat supraharmoniset päästöt sähkökäytöissä

Sähkötekniikan diplomityö

2023

80 sivua, 60 kuvaa ja 3 liitettä

Tarkastajat: Professori Pasi Peltoniemi ja diplomi-insinööri Ville Forsström

Avainsanat: Supraharmoniset, yliaallot, taajuusmuuttaja

Supraharmonisista yliaalloista on tullut uusi haaste taajuusmuuttajien valmistajille, sillä nämä aiotaan ottaa huomioon tulevissa standardeissa lähivuosina. IEC:n työryhmä (SC77A WG1) on valmistelemassa tulevaa IEC 61000-3-10 -standardia, jonka pääasiallinen tarkoitus on määritellä jännite- ja virtaharmonisten suurimmat sallitut arvot 2–9 kHz taajuusalueella sähkölaitteille, joiden nimellisvirta on enintään 75 A.

Tämä diplomityö antaa yleiskatsauksen tulevasta standardista, tarkastelemalla standardia valmistelevan työryhmän laatimaa luonnosta. Työn käytännön osuudessa suoritettiin johtuvien supraharmonisten (2-9 kHz) päästöjen mittauksia neljälle eri taajuusmuuttajalle erilaisissa ajopisteissä. Mittaustulosten perusteella kyseisten taajuusmuuttajien jännite- ja virtapäästöt pysyivät IEC 61000-3-10 enimmäisrajojen alapuolella.

Mittausten aikana selvitettiin myös saatavilla olevien mittalaitteiden käytännön soveltuvuus kyseisiin mittauksiin. Selvitysten perusteella mittalaitteilla pystyy tutkimaan taajuusmuuttajien supraharmonisia päästöjä, mutta standardissa määritetyn uuden ryhmittelymenetelmän puuttumisen takia mittalaitteilla ei pystynyt vielä suorittamaan virallisia vaatimuksenmukaisuusmittauksia.

ACKNOWLEDGEMENTS

I would like to thank Kari Ahlskog and Ville Forsström from ABB Drives for giving me the opportunity to research this interesting topic, and for coaching me throughout this thesis journey.

I also want to thank Pasi Peltoniemi, Juhamatti Korhonen and Aleksi Mattsson from LUT University for not only supervising and guiding me during this thesis, but also for the interesting power electronic courses they taught during my Master's studies at LUT University.

A special thank you also goes to my colleagues at the ABB Drives R&D laboratory for helping me with all kinds of practical problems in the laboratory.

Finally, I would like to thank my partner, Sara, for supporting me throughout my Master's studies.

Espoo, July 2023

Jukka Salonen

Table of contents

Abstract

Acknowledgements

1 Introduction 8
2 Harmonics in power drive systems 11
2.1 Harmonic generation in VSDs 11
2.2 Common methods for mitigating harmonics in VSDs 14
2.3 Harmonic analysis 15
2.4 Important existing EMC standards for PDS 17
2.4.1 IEC 61800-3 18
2.4.2 IEC 61000-3-2 and IEC 61000-3-12 18
2.4.3 CISPR 16 19
2.4.4 IEC 61000-4-7 19
2.5 Recent studies on supra-harmonics caused by VSDs 22
3 IEC 61000-3-10 23
3.1 General information 23
3.2 Artificial mains network 24
3.3 Limits for voltage and current emissions on 50 Hz systems 25
3.4 Signal analysis 27
3.5 Requirements for measurement and simulation 28
3.6 Informative annexes 29
3.7 Implementation of the AMN for testing purpose 30
3.7.1 General layout 30
3.7.2 Impedance characterization 32
4 Simulations against emission limits 35
4.1 Simulation model in Simplorer 35
4.2 Acquiring and processing of simulation data 37
4.3 Results with basic model 38
4.4 Results with the 150 m motor cable model 40

4.5 Conclusions for simulations 45
5 Laboratory measurements against emission limits 47
5.1 Testing facility and equipment 47
5.1.1 Tektronix MDO4104-3 oscilloscope 48
5.1.2 Yokogawa WT5000 power analyzer 49
5.1.3 Rohde & Schwartz ESW EMI test receiver ESW8 51
5.2 Drive A 52
5.2.1 Tests with a 5 m motor cable 52
5.2.2 Tests with a 150 m motor cable 56
5.3 Drive B 60
5.4 Drive C 61
5.4.1 Tests with a 5 m motor cable 62
5.4.2 Tests with a 100 m motor cable 64
5.5 Drive D 66
5.5.1 Without external AC choke 67
5.5.2 With external AC choke 68
5.6 Drive B under load conditions 71
5.7 Conclusions for measurements 74
6 Conclusions 77
References 79

Appendices

Appendix 1. Tested variable speed drives

Appendix 2. Drive B measurements with load

Appendix 3. Current harmonics of Drive A with 150 m motor cable, simulation vs actual measurement comparison

1 Introduction

This Master's thesis reviews the upcoming International Electrotechnical Commission (IEC) 61000-3-10 standard regarding supra-harmonic frequencies between 2 to 9 kHz and investigates whether it is possible to perform compliance measurements for the new standard for selected variable speed drives (VSD) with available measuring instruments. The main goal of this thesis work is to investigate if the selected drives would be compliant with the limits that the new standard draft proposes. Laboratory measurements showed that the voltage and current harmonic emissions of the VSDs remained below the limit lines specified by the standard draft and would therefore be compliant.

The increasing use of modern grid-connected power electronic converters has resulted in a rise in disturbance in the frequency range of 2-150 kHz, according to Davari, Hoene, Zare & Blaabjerg (2018) and Meyer, Khokhlov, Klatt, Blum, Waniek, Wohlfahrt & Myrzik (2018). Conducted emissions in this frequency range, commonly known as supra-harmonics or low-frequency electromagnetic interference (EMI), can degrade the power quality of electrical distribution systems. This can lead to issues such as the overheating of transformers and malfunctions in EMI-sensitive devices. Additionally, technologies that employ communication in the 2 kHz to 150 kHz frequency range (intentional emission sources) are increasingly being used. Emissions from grid connected converters (non-intentional emission sources) can interfere with the signaling frequencies of these communication systems. This interference can lead to significant malfunctions within the communication network. Such disturbances are becoming more frequent. (Davari, et al. 2018; Meyer, et al. 2018)

The standardization bodies have divided the 2-150 kHz range into two main frequency bands, 2-9 kHz and 9-150 kHz, in order to classify different types of electronic systems, as there are differences such as switching frequency ranges. While emissions under 2 kHz and over 150 kHz frequency range are extensively covered with several standards, the frequency range of 2-150 kHz lacks general standards as shown in Figure 1. (Davari et al. 2018)

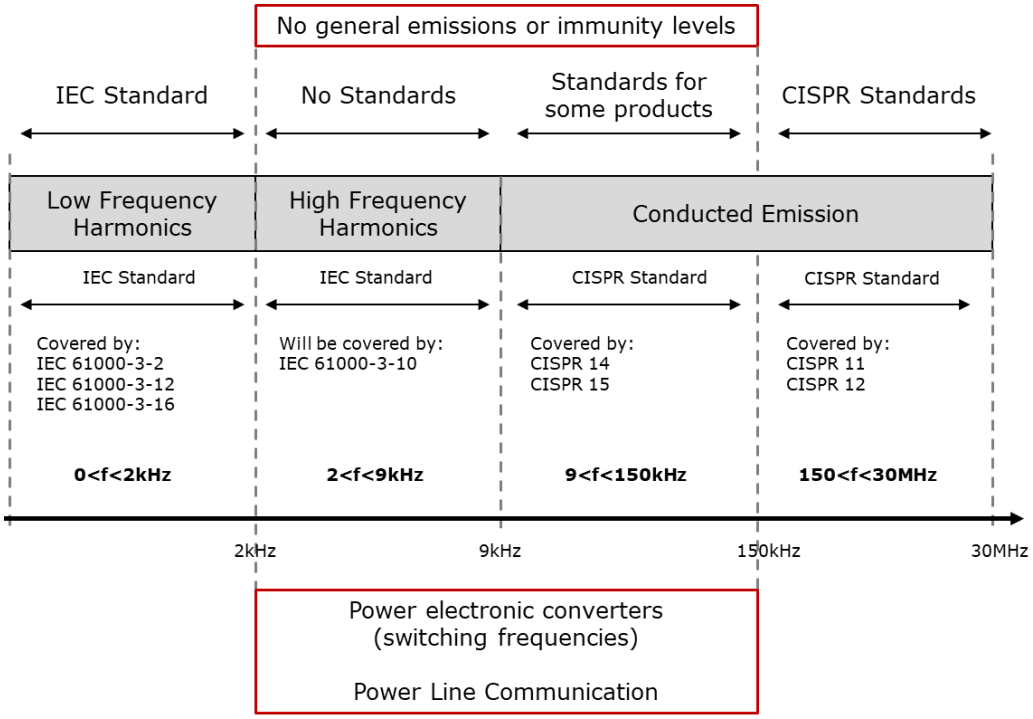

Figure 1: Conducted emission frequency ranges and applicable standards (modified from Davari, et al. 2018)

As seen in Figure 1, communication within power lines typically overlaps with the switching frequency range of power electronic converters. This emphasizes the importance for new standards addressing this frequency range.

Supra-harmonics have become a concern for network operators due to the lack of coverage in existing standards, according to Moradi, Zare, Kumar, Yaghoobi, Sharma & Kroese (2022a). This has prompted standardization committees to develop new standards to address this issue. VSD manufacturers must ensure that their products comply with any new standards from these standardization committees. As a result, the analysis of supra-harmonics has become an interesting subject for network operators, standardization committees, and VSD manufacturers (Moradi et al. 2022a).

A draft document of the upcoming IEC 61000-3-10 standard, which specifically addresses the 2-9 kHz range, is a key component of this thesis. The standard is being developed by Working group 1 of subcommittee 77A (SC77A WG1) within the IEC, and the document has been obtained from the group. The laboratory tests carried out in this work will adhere

to this draft document, thereby limiting the frequency range examined in this study to 2-9 kHz.

The practical aspect of the work was carried out at ABB Drives, in Helsinki. Drives A to D, listed in Appendix 1, were tested against emission limits proposed in the new standard at a dedicated electromagnetic compatibility (EMC) laboratory. The suitability of the WT5000 power analyzer and the ESW8 EMI receiver for the measurements in question are also evaluated. Each VSD is tested with an unloaded motor. In addition, Drive B is tested with different motor loads. Drive A is also tested by simulation. The simulation is performed with ANSYS Simplorer, where the real control programs of the drives can be modelled.

The structure of this Master's thesis is as follows: Chapter 2 outlines the principles of a harmonics generated by VSDs and includes information on mitigating methods. Chapter 2 also introduces the most significant active EMC standards and presents recent studies on the emissions from VSDs in the 2-9 kHz range. Chapter 3 introduces the new standard for the 2-9 kHz range and presents a prototype of the Artificial Mains Network (AMN) that was implemented for laboratory testing. Chapter 4 details the simulations conducted on Drive A. Chapter 5 discusses the laboratory measurements. Finally, Chapter 6 summarizes and concludes the thesis.

2 Harmonics in power drive systems

This chapter discusses the basic principles of harmonics and their generation in power drive systems (PDS) as a result of VSD operations. In addition, a brief overview of common existing EMC standards for PDS is provided. At the end of this chapter, recent studies on harmonics specifically caused by VSDs in the 2-9 kHz range are discussed.

A PDS is an integrated electrical and mechanical system designed to control the speed and torque of an electric motor. According to IEC (2021), a PDS basically comprises a VSD and an electric motor, along with auxiliary equipment such as motor shaft sensors and converter protection devices but does not encompass the supply transformer or the equipment driven by the motor (IEC 61800-2, 2021).

The structures and operations of VSDs and other power electronic converters are a significant area of study, featuring numerous textbooks and scientific publications. Popular works that explore these subjects in depth include “Fundamentals of Power electronics” written by Erickson & Maksimović (2020) and "Power Electronics: Converters, Applications, and Design" written by Mohan, Undeland & Robbins (2003), which provide comprehensive examinations of these topics.

For an in-depth investigation of harmonics, the book "Power System Harmonics" by Arrillaga & Watson (2003) is highly recommended. This reference work examines a range of topics related to harmonics, including harmonic analysis through techniques such as Fourier and related transforms, window functions and filter design strategies.

2.1 Harmonic generation in VSDs

The majority of power electronics applications involve a conversion of a 50 Hz or 60 Hz sine wave AC voltage to a DC voltage. As the trend is to employ cost-effective diode rectifiers for uncontrolled conversion of input AC to DC, a significant portion of power electronics applications, such as the rectifiers in VSDs, rely on diode rectifiers. An alternative common method for the AC-to-DC conversion involves the use of controlled rectifiers, which typically employ thyristors or insulated-gate bipolar transistors (IGBTs).

Controlled rectifiers provide the ability to regulate the output voltage and power flow, which can contribute to improved efficiency and performance. (Mohan et al. 2003)

VSDs produce harmonic emissions to the supply network mostly due to the presence of non-linear semiconductor components, like diodes, thyristors and IGBTs, within the rectifier circuit. Due to the non-linear current-voltage characteristics of rectifiers, VSDs draw non-sinusoidal current from the supply. The most common rectifier configuration in three-phase VSDs is a 6-pulse diode bridge rectifier. An example of a 6-pulse diode bridge rectifier and a non-linear current are illustrated in Figure 2:

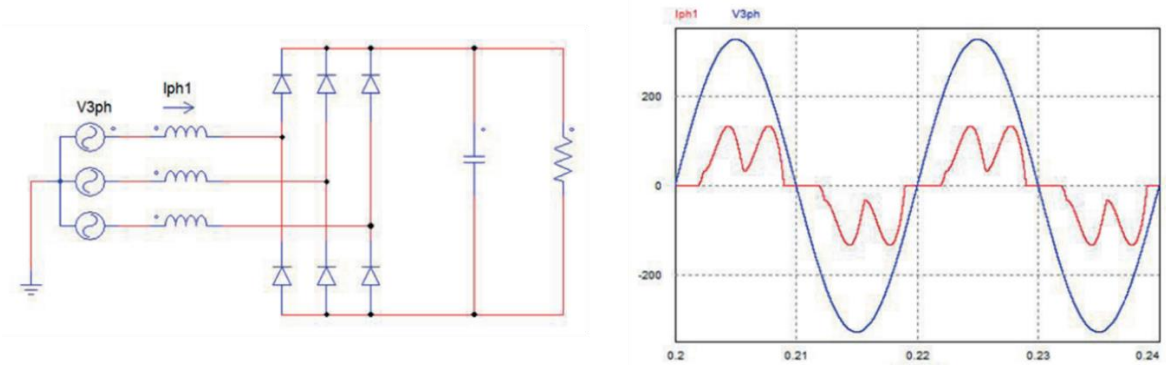

Figure 2: 6-pulse diode bridge rectifier, linear voltage and non-linear current (modified from Pinyol 2015)

Voltage distortion is produced as the non-sinusoidal currents, produced by non-linear loads, pass through the impedances of the system. The transformer secondary, which provides power to the rectifier and also to other connected loads, is typically referred to as the point of common coupling (PCC). Consequently, other loads connected at the PCC are affected by this distorted voltage. The extent of distortion is influenced by the power supply's stiffness, determined by the nominal power and impedance of the transformer. The power supply's stiffness is typically evaluated by short circuit ratio (R_{SC}), representing the ratio of available short-circuit current to the rated full load current. (Rockwell Automation 2014)

The distorted waveform causes various disturbances in the PDS such as the overheating of motors and cables. In addition, the disturbances not only affect the PDS but also extend to other electrical devices connected to the PCC. Typical issues arising from these disturbances

include malfunctions and disruptions in system components, as well as a shortened useful life of components due to the accelerated aging of insulation. Additionally, series and parallel resonances may amplify harmonic levels. (Arrillaga & Watson 2003)

The operation of rectifier creates harmonic frequency components that are multiples of the fundamental frequency. In a three phase 6-pulse rectifier, the characteristic harmonics that mainly occur are odd multiples of the fundamental frequency, which appear in the following order:

$$n = 6k \pm 1 \qquad (1)$$

where n is the harmonic order, and k is an integer (k = 1, 2, 3, ...).

Therefore, a 6-pulse rectifier primarily generates odd harmonics (n = 5, 7, 11, 13, 17…) while even harmonics are typically much lower or negligible. The 3rd harmonic and its multiples will not circulate in the system if the VSD is a three-phase, three-wire device. In a 50 Hz network a 250 Hz (5 x 50 Hz) waveform represents the 5th harmonic, a 350 Hz (7 x 50 Hz) waveform is the 7th harmonic, and so forth. (Peeran & Cascadden 1995)

When harmonics are summed with the fundamental waveform, they form a periodic non-sinusoidal distorted waveform, as illustrated in Figure 3.

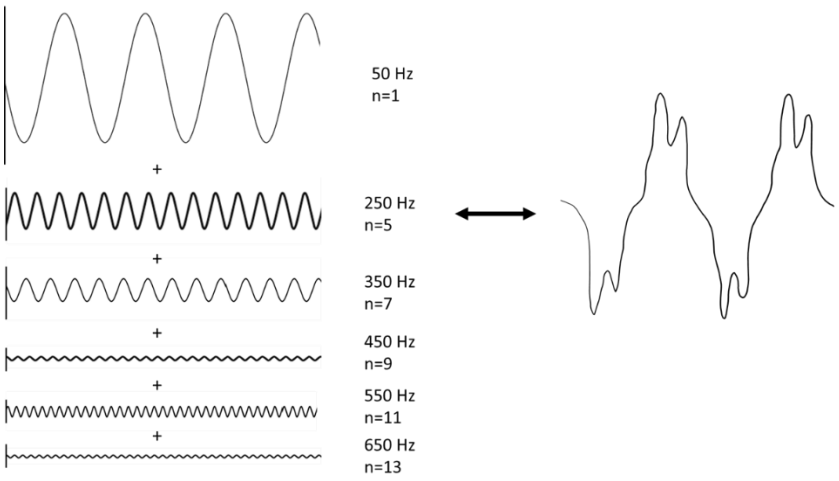

Figure 3: Distorted waveform consists of the fundamental waveform and harmonics (modified from Csanyi 2010)

The waveforms illustrated above are represented in the time domain. When examining the sum of sinusoids (distorted waveform) in the frequency domain using the Fourier transforms, the magnitude of individual harmonic components can be determined. A brief introduction to the Fourier transforms is provided in Section 2.3

Spectral components which are non-integer multiples of the fundamental frequency, that fall between each harmonic order, are called interharmonics. The input and output components of a VSD, the rectifier and the inverter, operate at different frequencies. Interharmonics are generated when these two systems with different operation frequencies are interconnected in the DC-link. Interharmonics can also be generated on the input side of the rectifier when the inverter output is unbalanced or when the drive is operating in overmodulation. (Das 2015)

Like harmonics, interharmonics can cause disturbances in the electrical system. Following the present standards, interharmonics are typically taken into account by merging them within harmonic components. This is called grouping.

Harmonic analysis traditionally focuses on determining harmonics (and interharmonics) up to the 40th order. As supra-harmonics are being investigated in this work, the harmonics under consideration span from the 40th to the 180th order (2-9 kHz). According to the notes in the IEC 61000-3-10 standard draft, the magnitudes of current harmonic components in the 2-9 kHz frequency range are expected to be between 0.1 and 50 mA.

2.2 Common methods for mitigating harmonics in VSDs

Reducing harmonics generated by VSDs can be achieved through several methods. Some of the widely used techniques include implementing following solutions:

- AC line reactors or DC chokes
- Active front end (AFE) drives
- Multi-pulse rectifiers
- Passive and active filters

AC line reactors and DC chokes are inductive components for harmonics mitigation. Both methods contribute to lowering the peak value of the input current. An AC line reactor

incorporates an inductor on the input side of the rectifier to reduce harmonics, while a DC choke is positioned within the DC-link between the rectifier and the inverter. Using AC line reactors or DC chokes with high enough inductance significantly reduces 5^{th}, 7^{th}, 11^{th} and 13^{th} harmonics.

AFE drives replace the conventional 6-pulse diode rectifier with a fully controlled IGBT bridge, resulting in an almost sinusoidal input current with minimal harmonic distortion. AFE drives significantly reduce harmonics of under 50^{th} order compared to conventional 6-pulse diode bridge drives. However, they generate increased harmonic magnitudes above the 50^{th} order. (ABB Drives 2017)

Multi-pulse rectifier configurations typically include 12-pulse, 18-pulse, and 24-pulse variations. These configurations effectively reduce harmonic distortion by employing multiple parallel 6-pulse rectifiers that feed a shared DC-bus. In 12-pulse rectifiers, the non-characteristic 5^{th} and 7^{th} order harmonics are relatively small, leaving only the characteristic 11^{th} and 13^{th} as well as the 23^{rd} and 25^{th} order and higher harmonics on the line side. 18-pulse drives mainly introduce the 17^{th} order and higher harmonics, while 24-pulse drives contribute the 23^{rd} order and higher harmonics to the system. (Peeran & Cascadden 1995)

Passive and active filtering methods are typically used for large industrial systems that contain multiple VSDs. Passive filters, which contain passive components, such as inductors and capacitors, are designed to filter certain harmonics to which they are tuned. Active filtering works by introducing harmonic distortion equal in magnitude but opposite in phase to the distortion created by the VSD, thereby restoring the waveform to a sinusoidal shape.

As the voltage distortion resulting from a specific current distortion is influenced by the R_{SC} of the power supply, harmonics can also be reduced by enhancing the supply. The higher the transformer's nominal power is, the lower the voltage harmonics will be. Similarly, the lower the transformer impedance, the lower the voltage harmonics become. (ABB Drives 2017)

2.3 Harmonic analysis

Harmonic analysis refers to determining the amplitude and phase of the fundamental frequency and its higher-order harmonics in a periodic waveform. This process produces the

Fourier series, which connects the time-domain function with its frequency-domain representation.

The magnitudes or RMS values of harmonic components can be determined by employing Fourier analysis on either the voltage or current waveform. The Fourier series of a periodically distorted waveform can be expressed using Equation 2:

$$x(t) = a_0 + \sum_{n=1}^{\infty}\left(a_n \cos\frac{2\pi nt}{T} + b_n \sin\frac{2\pi nt}{T}\right) \quad (2)$$

where a_0 is the DC component (average value) of the waveform $f(t)$, and a_n and b_n are the harmonic coefficients of the series, with *n* being the harmonic order. The variable *T* represents the interval or period during which the function repeats itself.

The DC component and harmonic coefficients of the series are given by:

$$a_0 = \frac{1}{T}\int_{-T/2}^{T/2} x(t)dt \quad (3)$$

$$a_n = \frac{2}{T}\int_{-T/2}^{T/2} x(t)\cos\left(\frac{2\pi nt}{T}\right)dt \qquad \text{for } n = 1 \rightarrow \infty \quad (4)$$

$$b_n = \frac{2}{T}\int_{-T/2}^{T/2} x(t)\sin\left(\frac{2\pi nt}{T}\right)dt \qquad \text{for } n = 1 \rightarrow \infty \quad (5)$$

As a common practice, Equations (3), (4), and (5) are expressed in relation to the angular frequency in the following manner (Arrillaga & Watson 2003, 20):

$$f(t) = a_0 + \sum_{n=1}^{\infty}[a_n \cos(n\omega t) + b_n \sin(n\omega t)] \quad (6)$$

$$a_0 = \frac{1}{2\pi}\int_{-\pi}^{\pi} f(\omega t)d(\omega t) \quad (7)$$

$$a_n = \frac{1}{\pi}\int_{-\pi}^{\pi} f(\omega t)\cos(n\omega t)\,d(\omega t) \qquad \text{for } n = 1 \rightarrow \infty \quad (8)$$

$$b_n = \frac{1}{\pi}\int_{-\pi}^{\pi} f(\omega t)\sin(n\omega t)\,d(\omega t) \qquad \text{for } n = 1 \rightarrow \infty \quad (9)$$

It is demonstrated by Arrillaga & Watson (2003, 20-22) that by utilizing the simplifications resulting from waveform symmetry that only contains odd-order harmonics and b_n coefficients (eliminating term a_n), Equation 10 can be derived:

$$b_n = \frac{8}{T}\int_{0}^{T/4} x(t)\sin\left(\frac{2\pi nt}{T}\right)dt \quad (10)$$

Equation 10 can be illustrated by a spectrum of amplitudes as demonstrated in Figure 4, showing the frequency spectrum of a square waveform. The amplitudes are inversely proportional to the harmonic order.

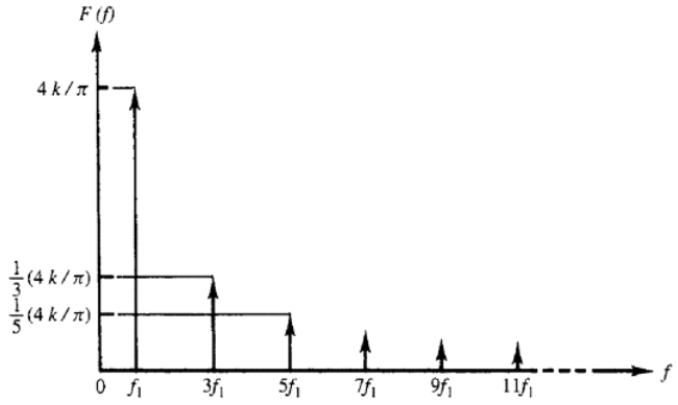

Figure 4: Harmonic spectrum of a square wave (Arrillaga & Watson 2003)

In real-world applications, measurement data is commonly available in a sampled discrete form, meaning that the data is represented by amplitudes separated by fixed time intervals. To analyze such data, Discrete Fourier Transform (DFT) is utilized. DFT is a vector-based calculation process operating on equally spaced data samples of a periodic signal that produces frequency vectors of the same length as the input time vectors. Computation of the frequency vectors from a large amount of time vectors is a slow process. Therefore, Fast Fourier Transform (FFT) is utilized for achieving a significantly faster transform of a function of time domain into a function of frequency domain. The FFT is developed from the DFT by reducing the amount of mathematical computations required, allowing the analysis of larger numbers of samples in a shorter amount of time. FFT is the foundation of modern harmonic and spectral analysis systems. (Arrillaga & Watson 2003, 17, 31, 35)

2.4 Important existing EMC standards for PDS

Limits for harmonics are specified in a several national and international standards. The IEC, based in Switzerland, is widely recognized as the authoritative body for electrical power quality standards. The IEC has established a series of standards known as Electromagnetic

Compatibility Standards to address power quality issues. These issues include harmonics and inter-harmonics, which fall under the category of conducted low-frequency electromagnetic phenomena. An additional significant standardization body is the Institute of Electrical and Electronics Engineers (IEEE), which is based in the US. (Arrillaga & Watson 2003)

2.4.1 IEC 61800-3

IEC 61800-3 is a product EMC standard that specifies EMC requirements for PDSs. The standard sets out different EMC requirements for VSDs based on their installation location. These locations are classified as either first environment (residential areas or places directly connected to a public low-voltage supply) or second environment (mostly industrial areas with their own transformers connected to a medium-voltage network). The standard also establishes four categories (C1 to C4) to classify VSDs based on their rated voltages and potential usage environments, with C1 being suitable for unrestricted use in residential areas and other similar environments. C2 is a more adaptable category, designed for use in industrial environments. C2 can also be used in residential areas if the equipment is installed by qualified personnel. C3, on the other hand, is designed exclusively for use in industrial environments. C4 is intended for high-voltage or high-current drives or those used in IT supply systems within complex settings in industrial environments. (IEC 2022)

2.4.2 IEC 61000-3-2 and IEC 61000-3-12

IEC 61000-3-2 and IEC 61000-3-12 are standards aimed at regulating the harmonic currents inserted into the public power grid by equipment. Specifically, IEC 61000-3-2 sets the rules for equipment drawing an input current up to and including 16 A per phase. On the contrary, IEC 61000-3-12 provides the guidelines for devices that have a rated input current exceeding 16 A and up to and including 75 A per phase. IEC 61000-3-2 and IEC 61000-3-12 set the boundaries for harmonic currents up to the 40^{th} order, which corresponds to 2 kHz for a fundamental frequency of 50 Hz. However, they do not provide any guidelines for frequencies in the range from 2 kHz to 9 kHz. (ABB Drives 2017)

2.4.3 CISPR 16

CISPR 16 serves as a basic standard series for electromagnetic compatibility. It is used by various product committees within the IEC as a reference for establishing EMC requirements for electrical products. Part 1-2 of the CISPR 16 series lays out the characteristics and operational performance required of equipment used for measuring radio disturbance voltages and currents. The frequency range in which these measurements are to be carried out spans from 9 kHz up to 1 GHz.

CISPR 16-2-1 covers conducted disturbance measurements, while CISPR 16-4-2 deals with uncertainties and limit modeling in measurement instrumentation. It is noteworthy that the CISPR 16 standard series does not define general conducted emission limits for the 2-150 kHz range. (IEC 2017)

2.4.4 IEC 61000-4-7

IEC 61000-4-7 is an important standard that covers the techniques for the testing and measurement of harmonics. One aspect that this standard details is the specific properties of the test setup's power supply. It establishes certain limits for the first 40 voltage harmonic components, ensuring the stability of the test voltage. The standard also outlines how to handle post-processing, particularly implementing grouping of the spectral harmonic and interharmonic components. These components are given at 5 Hz frequency intervals using a Fourier analysis on a 200 ms time window of the measured signal. The time window corresponds to 10 fundamental periods of a 50 Hz system (12 for a 60 Hz system).

Grouping involves summing together spectral components around harmonic frequencies. For instance, with a 50 Hz system at the 5^{th} harmonic, the summation extends to spectral components from 225 Hz to 275 Hz. However, only half of the values from the 225 Hz and 275 Hz frequency components are included in the calculations. The other halves are part of the adjacent groups of the preceding and following harmonic orders. The process of grouping adjacent spectral components results in an increased value of the harmonic. As an example, Figure 5 illustrates the grouping of the 5^{th} harmonic with adjacent interharmonics. (ABB Drives 2017)

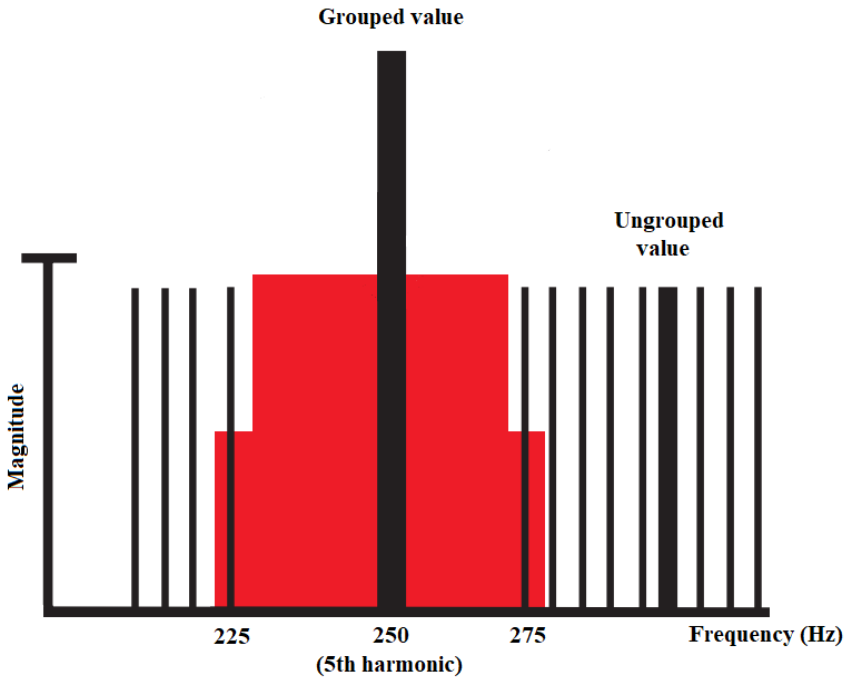

Figure 5: Illustration of IEC 61000-4-7 grouping (modified from ABB Drives 2017)

The IEC 61000-4-7 standard is particularly noteworthy due to its Annex B, introduced in 2002, which presents a tentatively defined guide on harmonic measurements up to 9 kHz. It has been utilized as a reference guide for conducting harmonic analysis within the 2 kHz to 9 kHz range. Annex B recommends the use of an Artificial Mains Network (AMN) in the test setup. The AMN's role is to standardize the impedance characteristics within the 2 to 9 kHz range, thereby ensuring the repeatability and reliability of the harmonic measurements for emissions evaluation. (IEC 2009)

The AMN, which is specifically inserted between the supply terminals and the Equipment Under Test (EUT) terminals, is crafted as per the standard's guidelines. Its construction involves specific resistance, inductance, and capacitance values. The magnitudes of these values are defined in the document. This configuration ensures the AMN's ability to consistently maintain the desired impedance characteristics across the frequency range.

Annex B introduces an alternative method for grouping spectral components. In this approach, the 5 Hz components are organized into center bands, each having a width of 200 Hz. For systems operating on a 50 Hz frequency, the frequency of the first band is 2100 Hz while the frequency of the last band is 8900 Hz, from which it follows that there are 35 bands

in total. The magnitude Y (current or voltage) of each band is the RMS value according to Equation 11:

$$Y_b = \sqrt{\sum_{f=b-95\ Hz}^{b+100\ Hz} Y_{Cf}^2} \tag{11}$$

Where *b* is the center frequency (e.g. 2100 Hz), which designates the band. Y_{Cf} is the current or voltage magnitude value of a specific frequency component. The frequency bands in the range of 2 to 9 kHz are illustrated in the standard as in Figure 6 below:

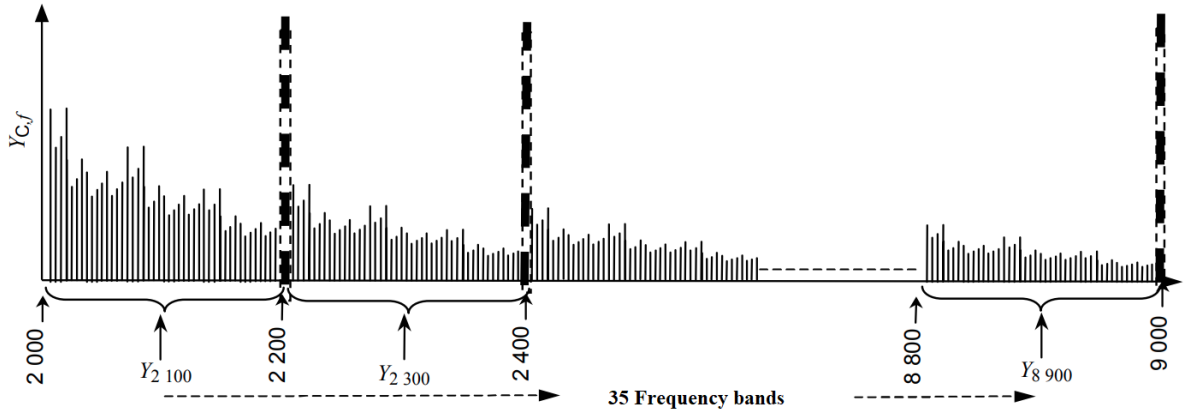

Figure 6: Frequency bands in the 2-9 kHz range illustrated in the IEC 61000-4-7 Annex B (IEC 2009)

Equation 11 and Figure 6 show that grouping of spectral components in the 2-9 kHz range differs from the grouping of the first 40 components that is shown in Figure 5. According to the IEC 61000-4-7, there is no need for high resolution in the frequency domain. Instead, the signal can be analyzed by grouping it into the aforementioned frequency bands.

An important point to note is that the standard does not specify emission limits for current and voltage harmonics. The emission limits are set to be defined in the IEC 61000-3-10 standard.

2.5 Recent studies on supra-harmonics caused by VSDs

Supra-harmonics is a relatively new concept so traditional textbooks do not contain much information on it. Even the standardization committees are waiting for measurement results and other studies from experts in the field, as mentioned in the IEC 61000-3-10 draft. Some recent studies on harmonics specifically caused by VSDs in the 2-9 kHz range have been published by the IEEE.

The article from Moradi et al. (2022a), studied the generation of 2-9 kHz current harmonics by VSDs in a multidrive network. The study analyzed various sources of current harmonics in a VSD and confirmed these findings through laboratory tests and simulations. One of the key findings of this study was that the 2-9 kHz current harmonics produced by a back-end inverter are dampened by the comparatively large DC-link capacitor of an VSD with a diode rectifier and a DC-choke filter. The 2-9 kHz current harmonics at the input of the tested VSD was primarily a result of the rectifier's switching function and DC-link ripples. (Moradi et al. 2022a)

The research also showed that the operation of other VSDs in a multidrive network could profoundly affect a VSD's current harmonics. An additional finding was that the utilization of a slim-DC filter in place of a DC choke leads to an increase in 2-9 kHz current harmonics within the multidrive network, which in turn can influence the harmonics of VSDs connected to the PCC. (Moradi 2022a)

In another recent study from Moradi, Farajizadeh, Zare, Kumar, Rathnayake, Sharma & Kroese (2022b), current ringing caused by an EMI filter is examined by developing a new mathematical model for VSD currents. It was found that current ringing primarily occurs due to a voltage difference across the capacitors in the EMI filter during changes in the commutation modes of the diode rectifier. It was further revealed that these current ringings can impact the input current harmonics of VSDs in the 2-9 kHz range. (Moradi et al. 2022b)

3 IEC 61000-3-10

A key resource in this work is the upcoming IEC 61000-3-10 standard that is being developed by the SC77A WG1. At the time of writing this thesis, a draft document of the standard is under review by industry experts. The standard defines testing methods, signal analysis and emissions limits for harmonics fed into the low-voltage network in the frequency range 2 kHz to 9 kHz (IEC 2023). This chapter examines the draft, outlining its main features and compliance requirements. The implementation of the Artificial Mains Network (AMN), utilized in the testing process, is also presented.

3.1 General information

The IEC 61000-3-10 standard is a forthcoming addition to the IEC 61000 series, which focuses on electromagnetic compatibility in electrical systems. Currently, the proposed standard is in the draft phase, indicating that the members of the committee are reviewing and gathering feedback on the draft. The final version of the standard is expected to be published in the near future, following the completion of the review and feedback process.

The standard is applicable to equipment with a rated apparent power of 1 kVA or higher. The maximum rated input current specified by the standard is 75 A. The voltage levels considered within the standard reach up to 240 V for single-phase systems and up to 690 V for three-phase systems.

The draft standard shares many similarities with the 5-page Annex B of IEC 61000-4-7. However, the draft introduces significant updates such as the proposed emission limits for current and voltage harmonics, rules for the measurement of harmonics, and their signal analysis. Furthermore, it provides additional schematic illustrations of the AMN implementation, and new guideline values for AMN impedance values in the 2-9 kHz range. The document also mentions the utilization of simulation in tests. (IEC 2023)

3.2 Artificial mains network

The standard draft defines an AMN with specified impedance values in the 2-9 kHz frequency range that can be used in compliance measurements. Using an AMN in the test setup ensures consistent impedance characteristics of the supply system and increases the reliability of the readings. Other EMC standards, like CISPR 16-1-2, also utilize the same methodology for conducted emission measurements for frequencies beyond 9 kHz.

When an AMN with impedance values according to the standard draft is used only the current needs to be measured. It is also allowed to perform measurements without an AMN. If AMN is not utilized, both voltage and current must be measured. (IEC 2023)

According to the measurement setup instructions of the standard, the AMN is placed between the supply and the EUT. Figure 7 illustrates the proposal by the standard committee for implementation of the AMN in 3-phase-3-wire systems, acting as a guidance model for building the frequency extension module.

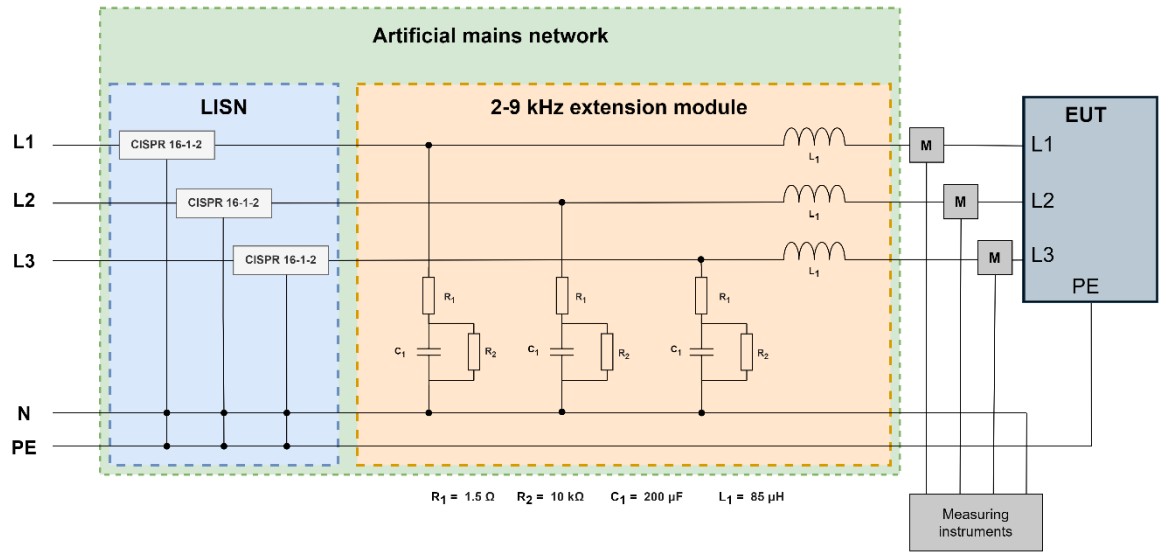

Figure 7: Diagram of the proposed AMN in a 3-phase measurement setup (modified from IEC 2023)

As seen in Figure 7, the AMN consists of a Line Impedance Stabilization Network (LISN) device that is commonly used in CISPR 16-1-2 compliance measurements, and a separate

frequency extension module which filters out additional interference and enables standardized measurements in the 2-9 kHz range.

In CISPR 16-1-2, different impedance values for several LISN types are specified. In the IEC 61000-3-10 draft, the intention is to utilize a basic model of LISN with an impedance of 50 Ω/50 mH + 5 Ω, covering a frequency range of 150 kHz to 30 MHz.

To verify the impedance characteristic of the implemented AMN within the range of 2-9 kHz, absolute impedance values are measured between each phase and neutral. For an AMN in a three-phase setup, the absolute value of impedance should follow Equation 12:

$$|Z| = 1{,}22 + 0{,}24 \times f + 0{,}02 \times f^2 \quad (12)$$

where f is frequency [Hz].

A ±20 % margin, within which the impedance values should fall, is provided for the values calculated using Equation 12. This margin is given to account for the tolerances of the components (their actual values).

3.3 Limits for voltage and current emissions on 50 Hz systems

In the draft standard, the emission limits for voltage harmonics in 2-9 kHz range are determined using two different equations. According to Equation 13, in the 2-3 kHz range, the upper limit for voltage spectrum components is 1% of the nominal voltage:

$$U_{\text{lim}} = \frac{U_{\text{n}}}{100} \quad (13)$$

where Un is nominal RMS phase voltage [V].

For the 3-9 kHz range, the logarithm of the level diminishes linearly with the logarithm of the frequency, as stated in Equation 14:

$$U_{\text{lim}} = 2.18 \times f^{-0.708} \times \frac{U_{\text{n}}}{100} \quad (14)$$

where U_{n} is nominal RMS phase voltage [V] and f is frequency [kHz].

For networks with U_{n} > 230 V, the current emission limit is determined by dividing the voltage emission limit by the AMN impedance value, as indicated by Equation 15:

$$I_{\text{lim}} = \frac{U_{\text{lim}}}{|Z(f)|} \tag{15}$$

where $|Z(f)|$ is the frequency-dependent AMN impedance value.

For networks with Un ≤ 230 V, the current emission limit is determined by Equation 16:

$$I_{\text{lim}} = \frac{U_{\text{lim}}}{|Z(f)|} \times \frac{230\,V}{U_{\text{n}}} \tag{16}$$

Voltage and current emissions are often represented in a logarithmic scale, specifically in a decibel scale, because it often provides a more convenient way to examine large numerical ranges. Equation 17 can be used to convert voltage values (V) into decibel microvolts (dBµV) or to convert current values (A) into decibel microamperes (dBµA):

$$Value_{\text{dB}} = 20 \times \log_{10}(Value) + 120 \tag{17}$$

where $Value$ represents the original current [A] or voltage [V] values and $Value_{\text{dB}}$ represents the conversion result in either [dBµA] or [dBµV] respectively.

Utilizing the aforementioned equations, it is possible to draw emission limit lines for both voltage and current, in dB units. The limit lines are presented in Figure 8.

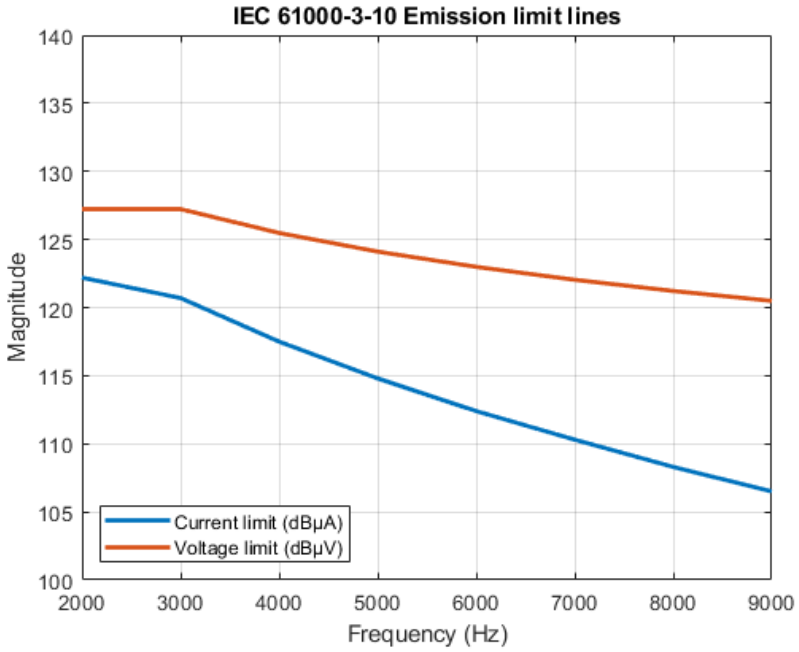

Figure 8: Voltage and current emission limit lines according to IEC 61000-3-10 draft

It is to be noted that the values illustrated in the graph are applicable for a condition where the RMS value of the phase voltage is nominally 230 V and the frequency is 50 Hz. These conditions apply to the laboratory measurements and simulations, the results of which will be compared with these emission limits.

3.4 Signal analysis

The guidelines for signal analysis in the standard draft share a strong resemblance with those in Annex B of IEC 61000-4-7. Like in the Annex B, for both voltage and current measurements, the draft recommends the use of a rectangular data acquisition window with a width of 200 ms, which corresponds to 10 fundamental periods for 50 Hz (or 12 for 60 Hz) systems. This leads to a frequency separation of 5 Hz between the consecutive measured current or voltage components, which are derived from the raw DFT.

Notably, the draft document mentions that the sampling frequency is not required to be in sync with the supply frequency. Given the low level of the signals to be measured, using a band-pass filter is suggested for reducing the measurement uncertainty. The band-pass filter attenuates the amplitudes of the fundamental and components above 9 kHz. The fundamental frequency attenuation should exceed 55 dB. All these aspects are also mentioned in Annex B.

The formula for grouping presented in the draft document is the same as that in Annex B (Equation 11), though it comes with certain refinements. The DFT outputs need to be grouped into 200 Hz bands, starting with the center band at 2100 Hz and ending with the center band at 8900 Hz, similar to what is suggested in Annex B of IEC 61000-4-7. A new aspect to note is that these bands should be spaced out by 5 Hz. Frequency steps of 5 Hz imply that there is an overlap of 195 Hz with adjacent bands. This results in a collection of 1360 Y_b values (instead of 35 values). (IEC 2023)

3.5 Requirements for measurement and simulation

In the final section, before the informative annexes, the measurement and simulation conditions are outlined. The text is somewhat unclear (e.g. referencing sections not yet present in the document), so it is expected to change in the next versions.

The draft standard mentions that the compliance with the standard can be determined by direct measurement or through validated simulation. These must be carried out with the equipment's operational controls adjusted to the mode that is predicted to generate the highest harmonic current emissions under normal operating conditions.

Requirements for the power supply of the test setup are similar to those outlined in section 5.4.2.3 of the IEC 61000-4-7 standard, which deals with equipment with an input current ranging from 16 A to 75 A. It outlines, for example, the following:

- The supply should provide a voltage equivalent to the rated voltage of the EUT
- The supply output voltage, frequency, and voltage unbalance must adhere to specified tolerances
- The harmonic ratios of the no-load output voltage must remain within defined limits for specific harmonic orders (e.g 1.5% for the 5^{th} harmonic and 1.25% for the 3^{rd} and 7^{th} harmonics), emphasizing that the supply source impedance should be kept low

In terms of the requirements for the measuring equipment, the requirements outlined in the standard IEC 61000-4-7:2009 are expected to be followed for both current and voltage instruments.

The requirements for simulation state that the simulation model needs to be validated in order to accurately represent the actual measurements. Therefore, laboratory measurements are still required. It is proposed that the validation is done using a product from the upper end of the power range, within the product range. The simulation results should not deviate by more than 10% from the actual measurement results. (IEC 2023)

3.6 Informative annexes

The draft standard concludes with informative annexes. Annex A discusses the relevancy of the 2-9 kHz measurement band, while Annexes B and C provide detailed examples of alternative constructions for the test setup, including different types of EUTs and more detailed schematics of the extension module.

Before the standard is officially published, there is an opportunity to gather more insights from the field and other information sources. At the time of writing this thesis, the committee is actively seeking documented feedback during this period.

In Annex A, the question is raised regarding the most suitable frequency band for testing products with the lowest switching frequency of 9 kHz. The discussion revolves around whether the 2-9 kHz frequency band should be included in testing or if the frequency range should start at 9 kHz, taking into account that harmonics can be identical or multiples of the switching frequency. The aim is to focus the measurements on relevant frequency bands, thereby saving both time and cost when ensuring compliance of a product.

The scarcity of data is highlighted, with minimal measurements demonstrating current emissions in this frequency range. It is also pointed out that academic research on conducted emissions often treats the 2-150 kHz band as a singular entity, potentially overlooking specific properties in the lower part of the band.

Annex A invites additional measurements from industry experts in the 2-9 kHz frequency band, which would help decide the necessity of measurements for compliance in this frequency range. Potential categorization of products based on factors such as their switching frequency and the probability of them generating oscillations in the 2-9 kHz band, is suggested. (IEC 2023)

3.7 Implementation of the AMN for testing purpose

This section describes the process of implementing the AMN, outlining the primary characteristics of the constructed frequency extension module prototype. The prototype had been assembled and its functionality preliminarily tested before starting this thesis work.

3.7.1 General layout

Figure 9 below depicts the circuit diagram of the AMN that was used in laboratory measurements, including how it is connected to the EUT.

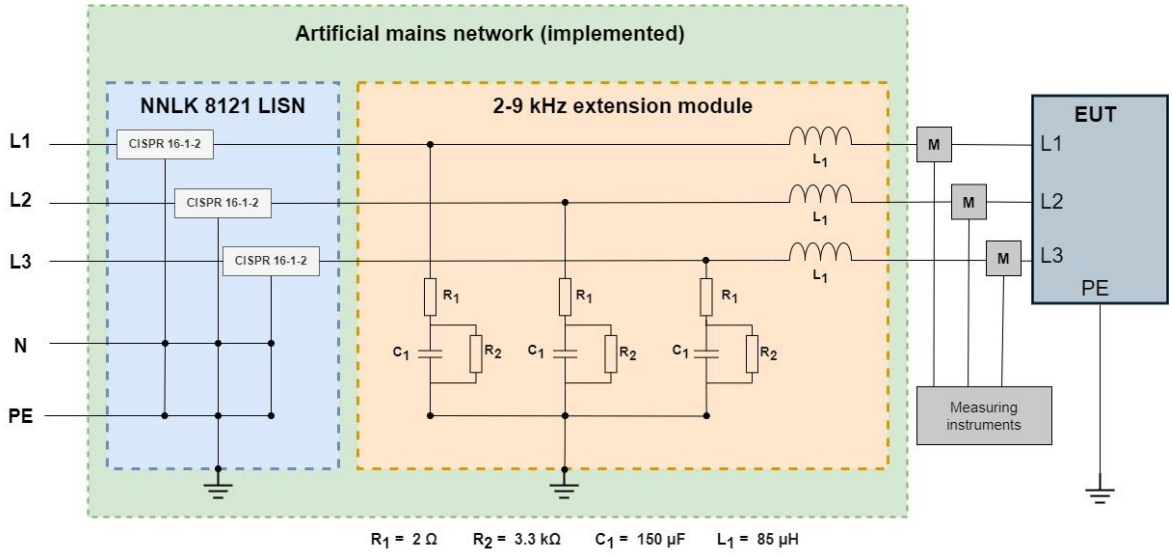

Figure 9: Circuit diagram of the AMN used in laboratory

The circuit diagram also shows the structure of the implemented frequency extension module, showing the locations and ratings of chosen components. The connection principle differs slightly from the draft proposal, as the grounding of the extension module is not implemented through the N conductors via the LISN, but rather through the star point. There are also minor differences in the component values.

The LISN device required in the test setup is a commercial artificial network device, which is typically employed in EMC tests as per the guidelines set out in the CISPR 16-1-2

standard. In this work, the NNLK 8121 LISN manufactured by Schwarzbeck was used as part of the AMN. According to Schwarzbeck, the device offers a mains connection to the EUT with a standardized impedance of 50 µH + 5 Ω. It also minimizes interference voltages originating from the mains. The LISN provides an extended frequency range of 9 kHz - 30 MHz. (Schwarzbeck 2023)

The supply voltage and the EUT should be connected to the LISN using the wing terminals, with the supply voltage connected at the back panel and the device under test connected at the front panel. The LISN is grounded to the metal floor of the electrical laboratory using a short and wide grounding strap, and also through the grounding conductor of the supply cable connected to the rear terminal.

By default, the NNLK 8121 LISN has a prefilter on the grid side, which consists of a 250 µH choke, 4 µF capacitor and a 100 kΩ resistor. This type of a filter is a typical feature for commercial LISNs that enables the extended frequency range of 9 kHz - 30 MHz. Due to the assumption in the IEC 61000-3-10 draft that the AMN implementation utilizes a basic model LISN (150 kHz - 30 MHz), the NNLK 8121 had to be modified by disabling the mentioned filter components from the circuit to comply with the specifications.

The frequency extension module prototype was specifically assembled in order to conduct tests in accordance with the IEC 61000-3-10 standard. Figure 10 shows a photograph of the implemented frequency extension module prototype.

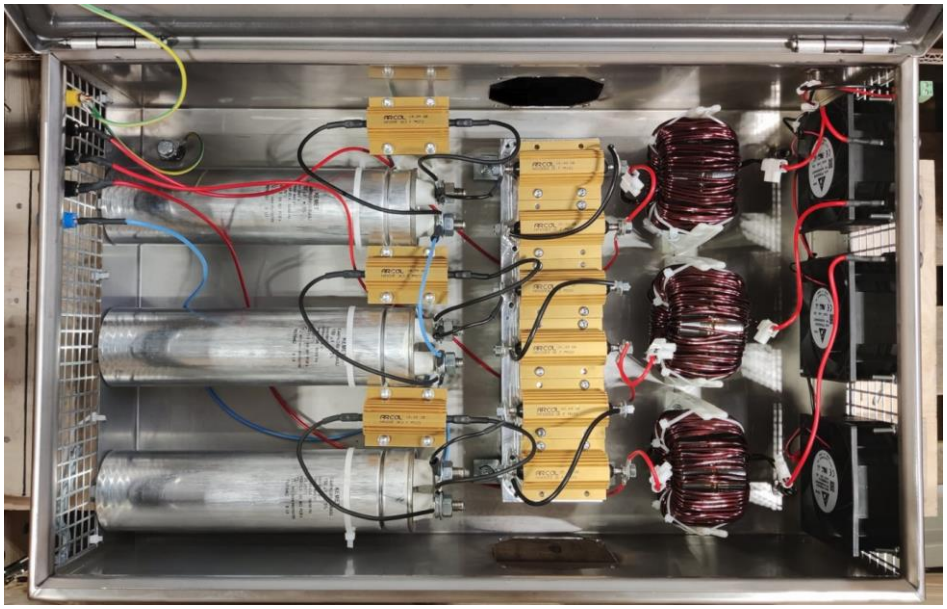

Figure 10: IEC 61000-3-10 frequency extension module prototype (chassis door opened)

The prototype is meant to be placed on the laboratory's metallic floor, allowing it to be grounded through the metal casing. Based on preliminary tests, the device was found to leak approximately 10 A of current to the ground, requiring significant cooling for its resistors. As a result, a total of 5 fans were installed in the prototype to circulate the air within the enclosure and to cool the resistor heat sink.

3.7.2 Impedance characterization

Before proceeding to the actual harmonics measurements, the impedance values of the AMN were verified with an impedance analyzer. The impedance verification measurement is shown in Figure 11.

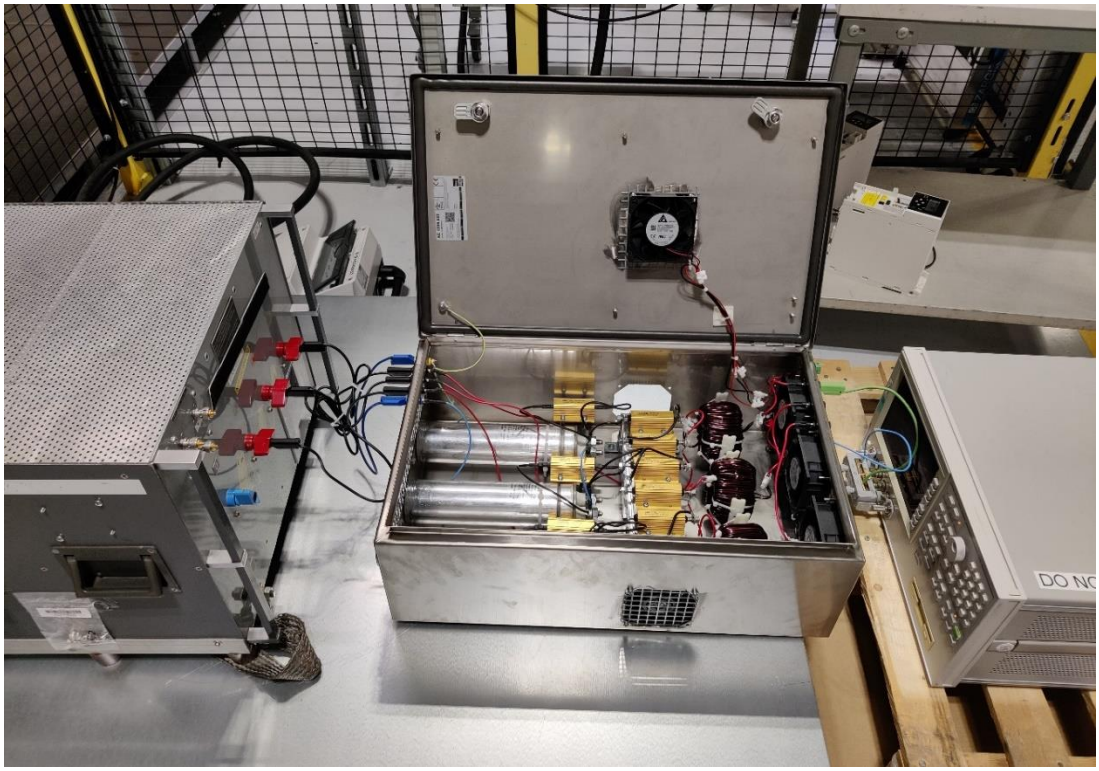

Figure 11: AMN impedance measurement setup

On the left side of the image, the CISPR 16-1-2 compliant LISN is placed, and in the middle is the prototype of the extension module with the chassis door open. The star point was connected to the chassis with an external conductor at the left-hand side of the extension module. On the right, an impedance analyzer used as the measuring instrument is placed.

The LISN and the module are positioned on a metallic plate serving as the reference level, that is floating. Floating the AMN is necessary in this measurement as otherwise part of the measurement current may leak back through the power supply of the impedance analyzer, forming a ground loop.

The impedance measurements were conducted between each phase and the floating reference level, one phase at a time. The results of these measurements are compiled in Figure 12.

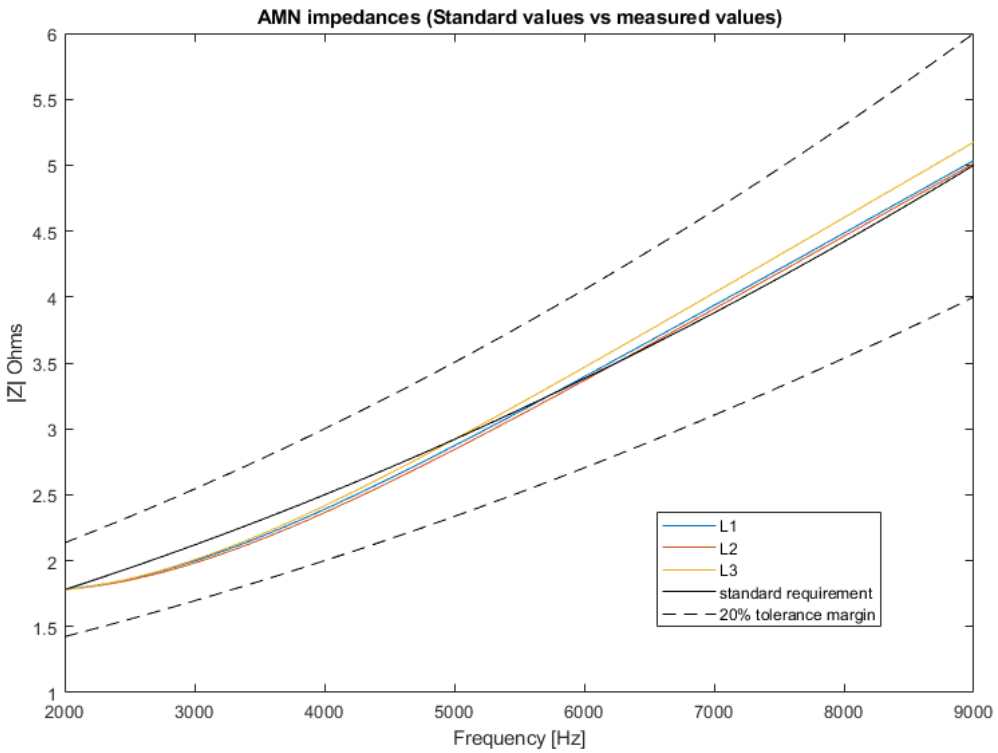

Figure 12: Measured impedance values versus standard values in the 2-9 kHz range

From Figure 12, it can be observed that the measured impedance values match relatively close the guideline values given in the draft standard (Equation 12). There is some allowance for deviation, as indicated by the dashed lines, which represent the margin within which these measured values should be.

4 Simulations against emission limits

One part of the work was to investigate how well the simulation of a VSD corresponds to laboratory measurement results and whether a pre-existing simulation model used by ABB could be used for compliance testing. Simulations were performed for a VSD model corresponding Drive A, that operated with an unloaded 37 kW induction motor.

Simulations were conducted first without a model for motor cables and by using different switching frequencies and motor speeds. Then simulations were conducted with a previously made 150 m long motor cable model. This chapter presents the results and conclusions from these investigations.

4.1 Simulation model in Simplorer

The simulations were carried out in the Simplorer simulation environment using Ansys Electronics Desktop 2020 R2 software. The software is a typical SPICE circuit simulator. An existing model was available for Simplorer, having a structure that included a 6-pulse diode rectifier, DC-link, DC-chokes and an inverter. The structure of the model was therefore like Drive A. The inverter's rated current, as well as the characteristics of DC-link capacitor and DC-choke, were set to match the specifications of Drive A. In addition, an EMI filter was added to the input side of the rectifier, to replicate the EMI filter specifications of Drive A.

An induction motor model was connected to the inverter. The motor characteristics were set to match the induction motor that was available for the laboratory measurements (37 kW / 400V). A model of the realized AMN was also constructed in Simplorer and incorporated into the simulation model between the supply and the rectifier.

By using this simulation model, the simulation aimed to replicate the characteristics and performance of Drive A in the laboratory measurements. Figure 13 shows the utilized simulation model in the Simplorer simulation environment. For visual clarity, certain measurement points required for the simulation have been omitted in the picture.

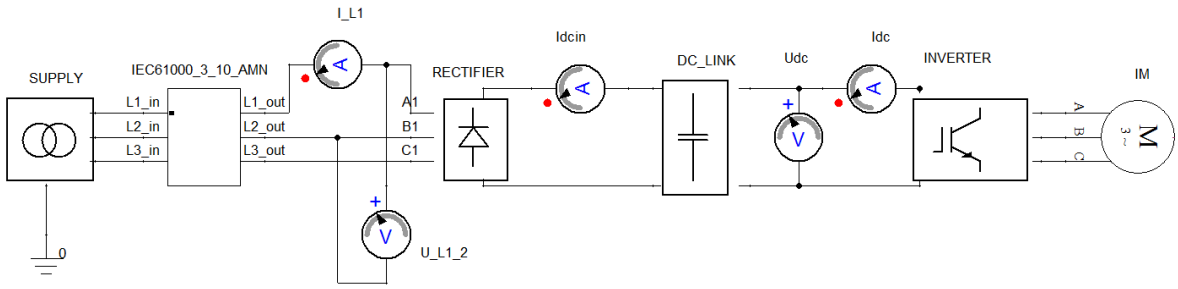

Figure 13: Simulation model in Simplorer

Figure 14 shows the structure of the AMN that was implemented in simulations, corresponding to the structure that is proposed in the IEC 61000-3-10 draft. It contains the CISPR 16-1-2 compliant LISN impedance (50 µH + 5 Ω) that is typically required in measurements for higher frequencies, as well as the frequency extension part.

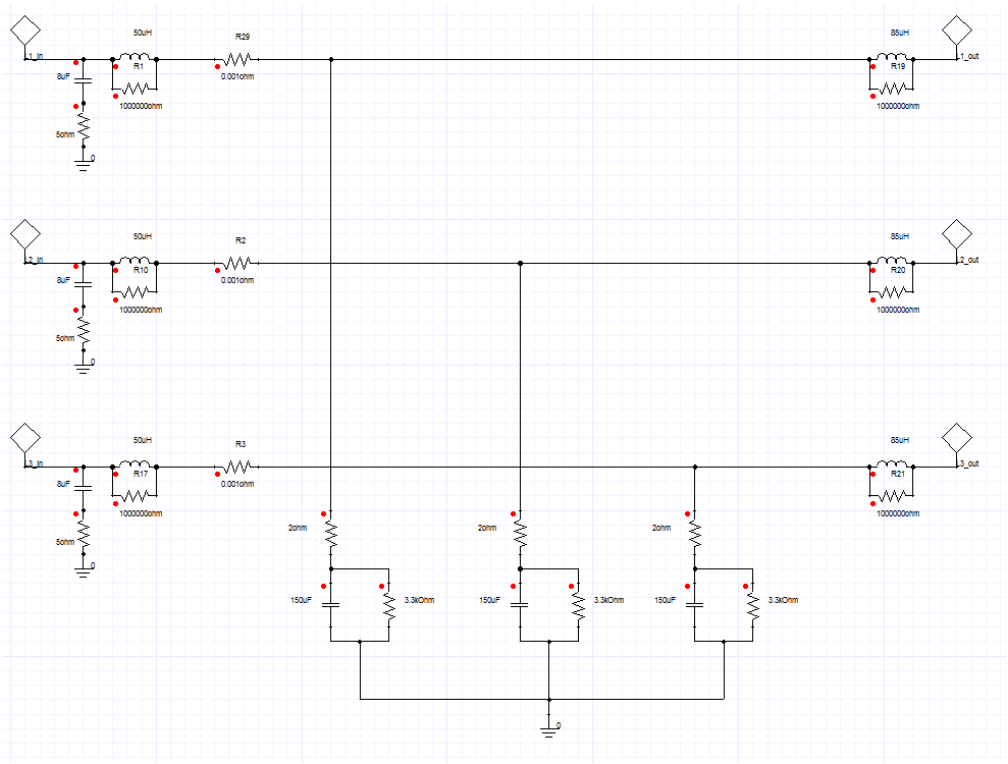

Figure 14: IEC 61000-3-10 AMN implementation in Simplorer simulations

The simulation model utilizes a dynamic link library file (DLL) that contains the code for motor control. Using measurement information, such as the motor currents and DC voltage, the code produces IGBT control signals for the inverter. The DLL file uses the same source code for the motor control functionality as Drive A, which was tested in this work in the laboratory.

4.2 Acquiring and processing of simulation data

The code inside the DLL file utilizes a time step of 250 ns. In Simplorer's settings, the minimum time step (Hmin) was set to 200 ns, while the maximum time step (Hmax) was set to 2000 ns. This results to having a variable sampling rate for the simulation. The simulation time was kept as short as possible (between 1 to 3.5 seconds) because it was found that the simulation model was computationally intensive and sensitive to initial conditions of load and control, which could lead to instability. However, it was ensured that the motor speed had sufficiently stabilized for at least a few hundred milliseconds, as a data acquisition window of 200 ms was required by the standard.

In the simulation, waveforms of the current of phase L1 (I_L1 in Figure 13) and the voltage between L1 and ground (U_L1_2) were recorded and exported as raw data in CSV files. Although the simulation program can perform Fourier analysis and present the results in the harmonic spectrum format, the results were processed manually in MATLAB using the data of CSV files.

Processing the measurement data in MATLAB offers more convenience. As the raw data is recorded with a variable sampling rate, interpolation is needed. Utilizing the *interp1()* function in MATLAB allows for adjusting a fixed time step and a constant sampling rate. In addition, MATLAB provides its own *fft()* function, enabling the presentation of the harmonics through it. The main reason for processing the data in MATLAB was that the simulation software did not offer the required grouping of harmonics. In MATLAB, the grouping of harmonics was calculated utilizing the method provided by the draft standard.

4.3 Results with basic model

As an example, the voltage and current waveforms recorded during the simulation are shown in Figure 15. The current and voltage waveforms are illustrated in the time domain, measured between the AMN and input of the rectifier. The current drawn by the DC capacitor is pulsed, meaning it contains harmonics. The current waveform is however relatively sharp, which may indicate that the simulation model is too simple or ideal.

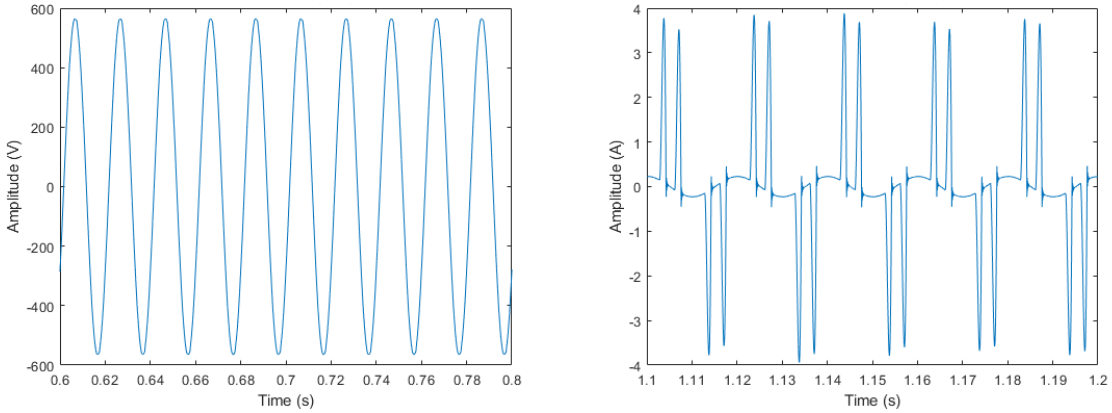

Figure 15: Simulated Drive A, voltage waveform (L1-L2) and current waveform (L1) in time domain (4.5 kHz, 510 rpm)

Figure 16 and Figure 17 show the voltage and current spectrums calculated from the exported data. The left-hand diagrams are obtained by first utilizing the fft() function in MATLAB, which calculates the spectrum magnitudes using an FFT algorithm. Then the magnitude values are converted in dBµV and dBµA scale, before plotting the diagrams. The right-hand diagrams are obtained utilizing the grouping function and dB scale conversion for the spectrum magnitudes obtained from the FFT. The red dashed line in the right-hand diagrams represents the limits calculated in Section 3.3

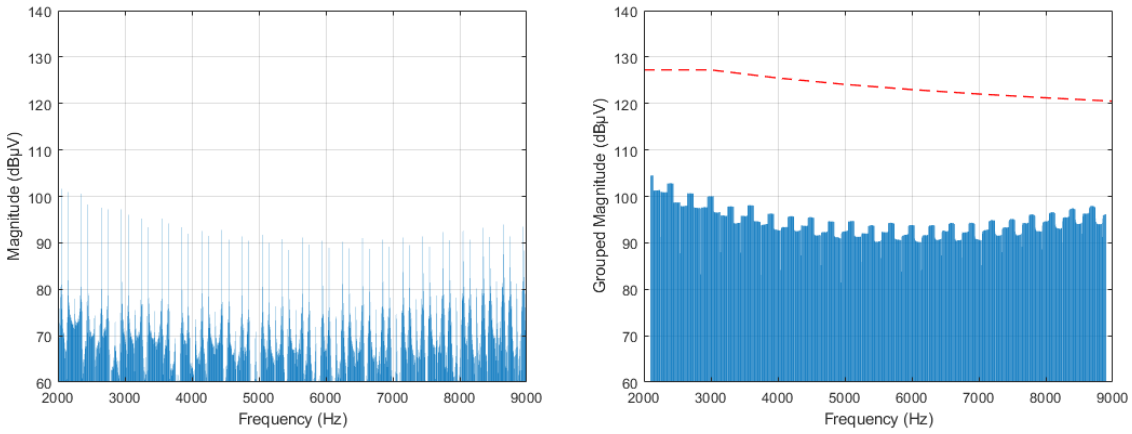

Figure 16: Simulated Drive A, voltage waveforms in frequency domain (4.5 kHz, 510 rpm)

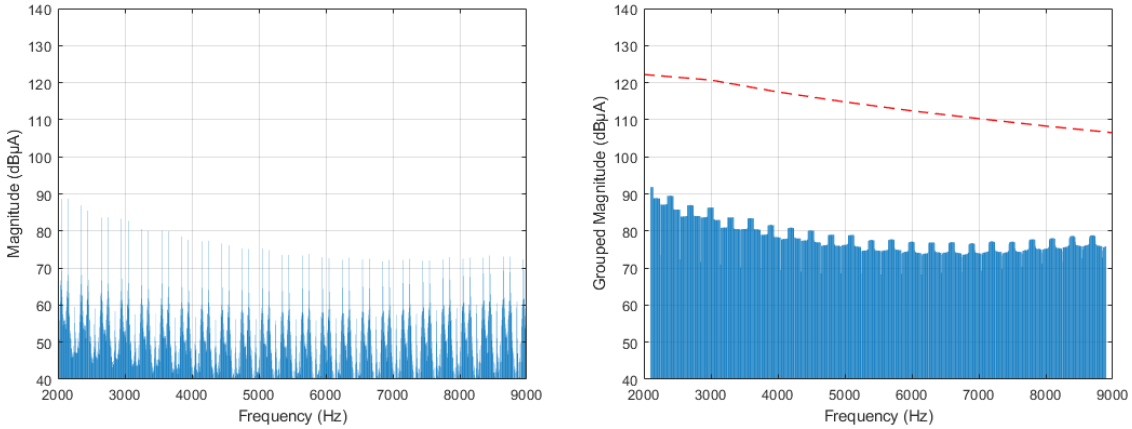

Figure 17: Simulated Drive A, current waveforms in frequency domain (4.5 kHz, 510 rpm)

By comparing the left and right diagrams of Figure 16 and Figure 17, the impact of grouping can be observed, as the final values that are compared against the limits are slightly increased. The diagrams indicate that according to the simulation of the basic model, the emissions are far from the limits in the 2-9 kHz range. However, the surprising issue is that there are no signs of the impact of the switching frequency in the simulation, which in this case might be expected to show as higher magnitudes near the switching frequency 4.5 kHz and its multiple 9 kHz. Changing the switching frequency or motor speed did not cause significant changes in these harmonic results.

4.4 Results with the 150 m motor cable model

The second set of simulations included the motor cable model. It is constructed according to cable capacitance measurements of a real 16 mm^2 MCCMK type cable. The motor cable model is based on a vector-fitting rational-function approximation, a methodology presented in an article written by Stevanović, Wunsch, Madonna and Skibin (2014). The motor cable model has previously been used for EMI simulations regarding frequencies up to 30 MHz. For simulations on this work, the cable model was placed between the inverter and motor, as shown in Figure 18.

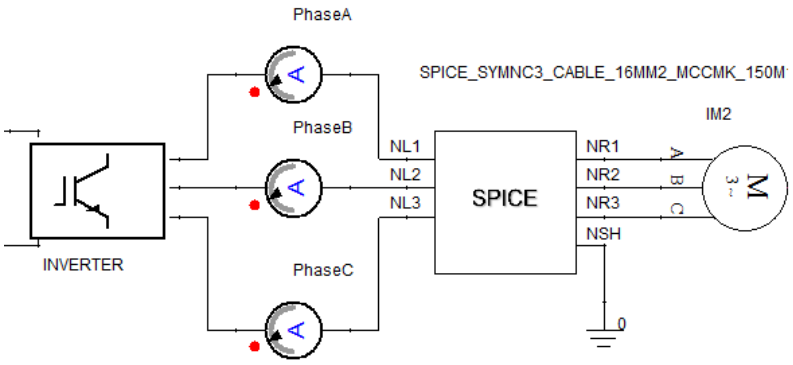

Figure 18: 16 mm^2 MCCMK (150 m) motor cable model

By including the model of a 150 m motor cable the simulation model became computationally heavier, extending the simulation time significantly. Due to the simulation model already being heavy and unstable (simulation process often getting stuck), comprehensive experiments were not feasible within the time constraints. However, simulations were still conducted for a 510 rpm motor speed with switching frequencies of 3 kHz, 4.5 kHz and 12 kHz.

As an example, the voltage and current waveforms recorded during the simulation are shown in Figure 19, illustrating the current and voltage waveforms in time domain, with 4.5 kHz switching frequency and a 510 rpm motor speed.

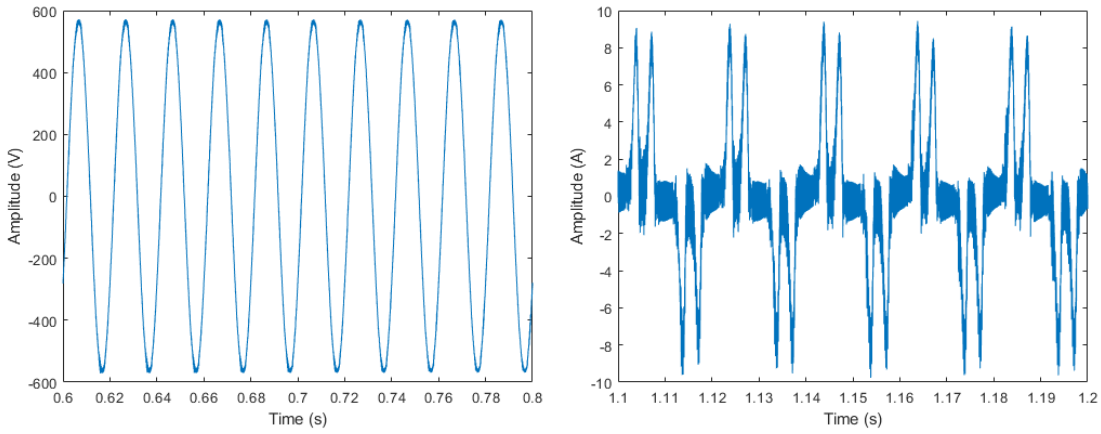

Figure 19: Simulated Drive A with the 150 m cable, voltage and current waveforms in time domain (4.5 kHz, 510 rpm)

When the simulation included the modeling of the 150 m motor cable, more distorted waveforms are observed in the time domain. The differences to the basic model (Figure 15) can be better observed by zooming in on the diagrams, as seen in Figure 20 and Figure 21. The left-hand diagrams show the waveforms in the basic model, while the right-hand diagrams show the waveforms in the 150 m motor cable model.

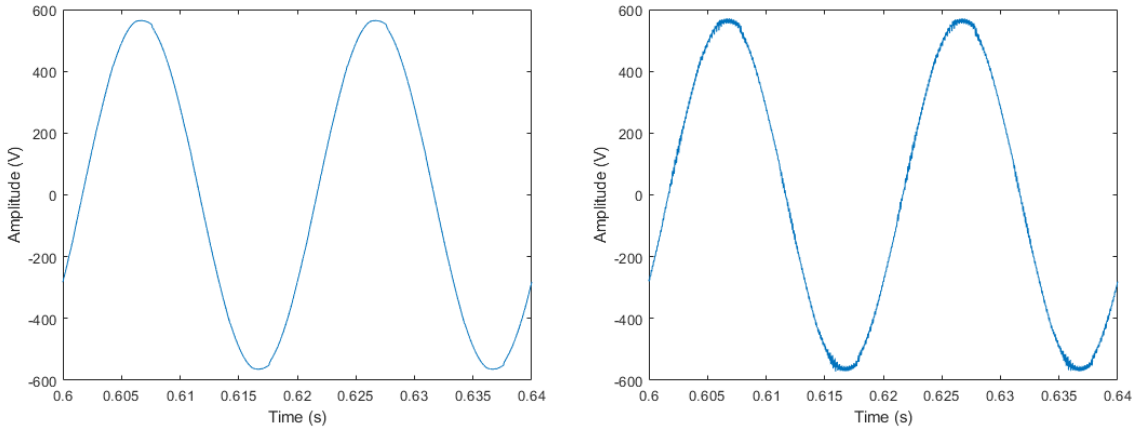

Figure 20: Zoomed in diagram of voltage, basic model vs 150 m cable model (4.5 kHz, 510 rpm)

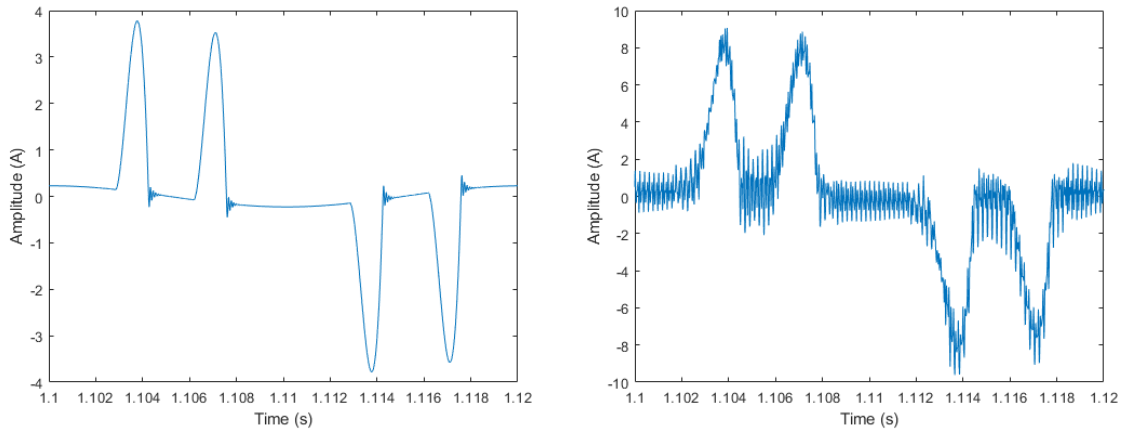

Figure 21: Zoomed in diagram of current, basic model vs 150 m cable model (4.5 kHz, 510 rpm)

In particular, the current waveform appears more distorted with the 150 m cable model. The amplitude of the current spikes is also roughly doubled.

Utilizing FFT for the exported data, diagrams in Figure 22 and Figure 23 are obtained. The diagrams present the voltage and current spectrums in ungrouped and grouped dB scale.

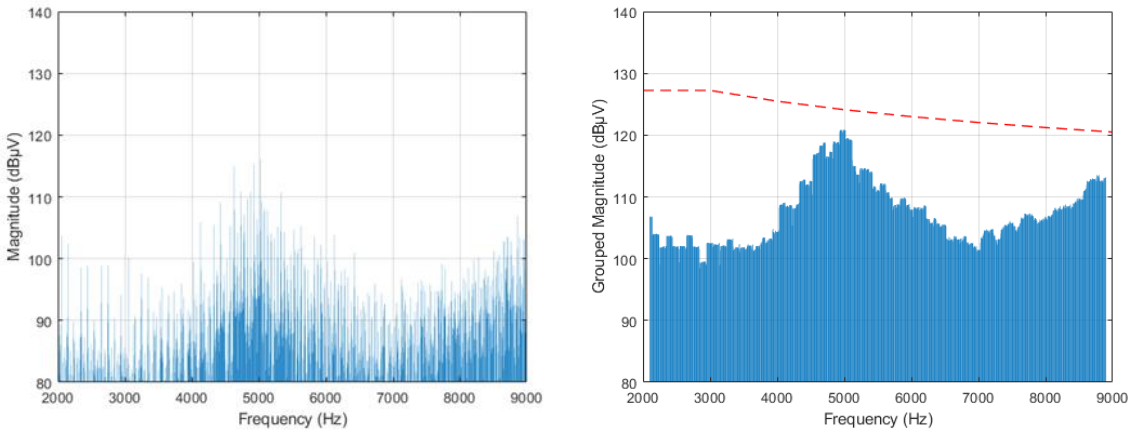

Figure 22: Simulated Drive A with 150 m cable model, voltage waveform in frequency domain (4.5 kHz, 510 rpm)

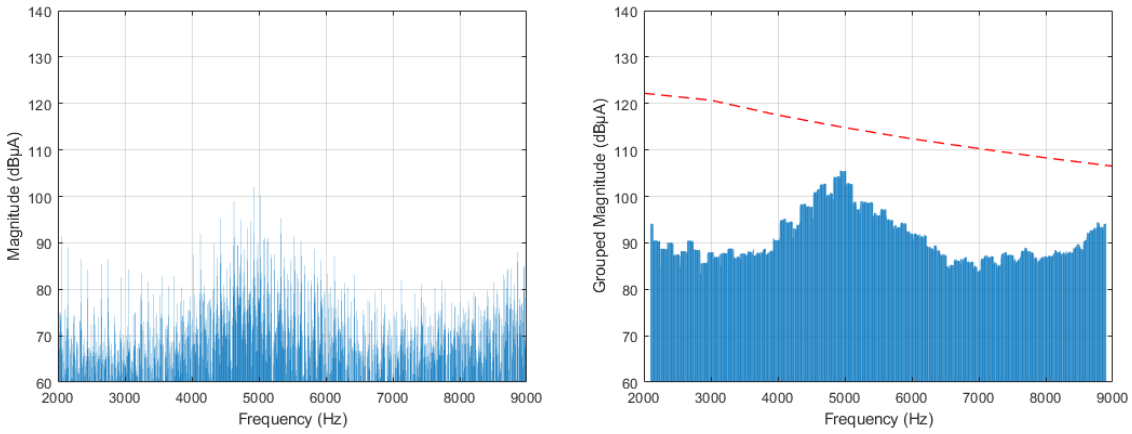

Figure 23: Simulated Drive A with 150 m cable, current waveform in frequency domain (4.5 kHz, 510 rpm)

The diagrams show the impact of having the 150 m cable model included in simulations. Higher magnitudes near the switching frequency and its multiple can be observed. There is, however, a slight offset from the switching frequency as the highest magnitudes can be found near the 5 kHz frequency. The difference from the highest point to the limit line is approximately 3.3 dBµV for the voltage and approximately 9.3 dBµA for the current.

Even higher frequency offset is displayed in Figure 24, presenting simulated current emissions with a switching frequency of 12 kHz. Although the grouped magnitudes are quite far from the limits within the 2-9 kHz range, significantly higher magnitudes are observed at approximately 13 kHz. This indicates that the simulation model still needs improvements to be more accurate.

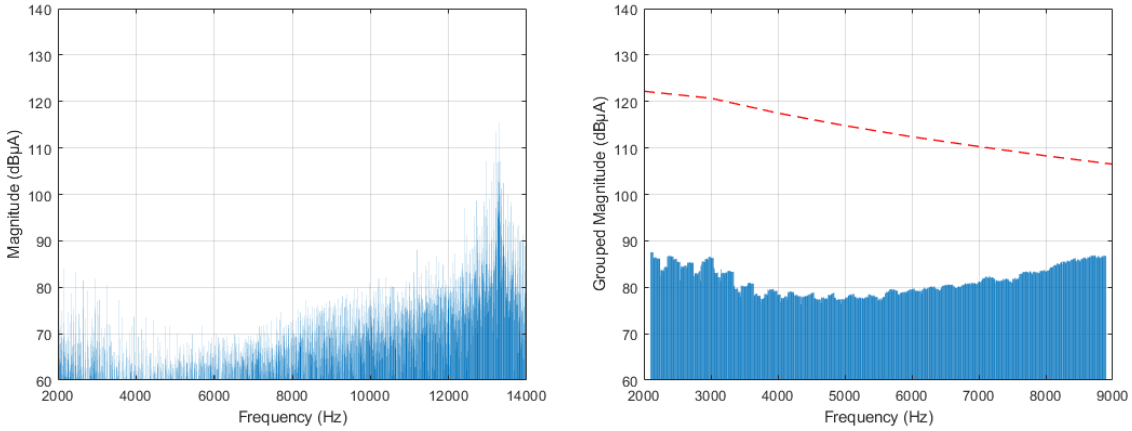

Figure 24: Simulated Drive A with 150 m cable, current waveform in frequency domain (12 kHz, 510 rpm)

On the other hand, with switching frequency of 3 kHz, the highest magnitudes are found closer to the switching frequency and its multiples, as presented in Figure 25.

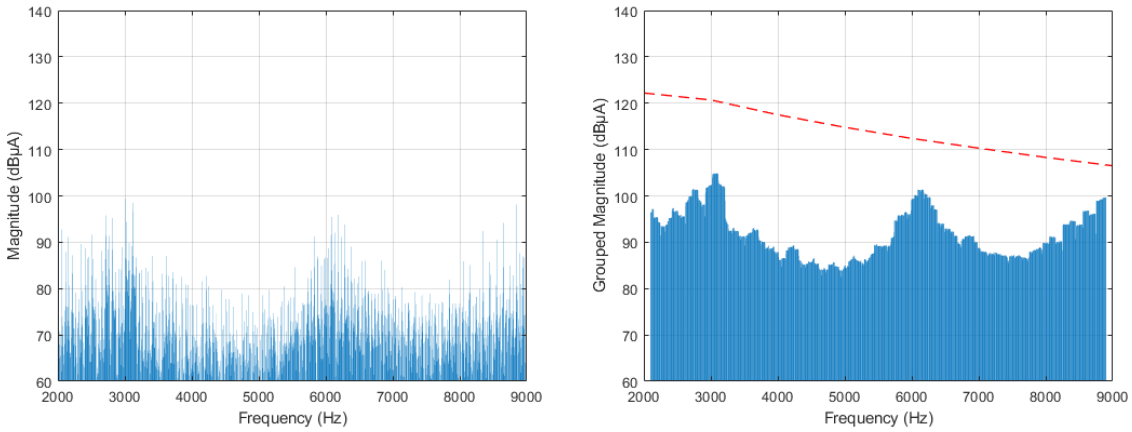

Figure 25: Simulated Drive A with 150 m cable, current waveform in frequency domain (3 kHz, 510 rpm)

A simulation with a 150 m motor cable was also attempted using a simpler method where the SPICE model was replaced by capacitors, which roughly represent real cable capacitances and have a similar frequency response for the 2-9 kHz range. The cable model utilizing just capacitors is shown in Figure 26.

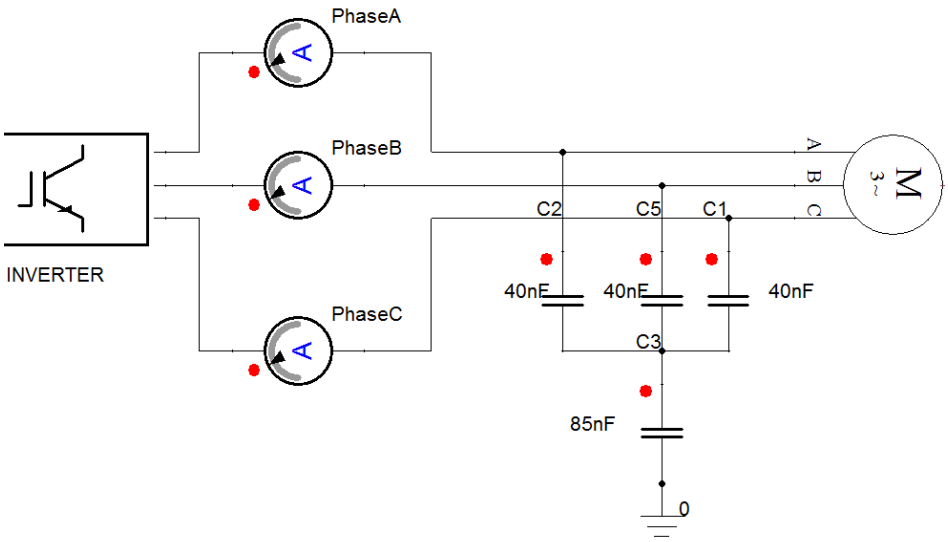

Figure 26: View in Simplorer, 150 m motor cable model using capacitors

The simulated currents for the 4.5 kHz switching frequency and 510 rpm motor speed, using the simpler motor cable modeling, is shown in Figure 27.

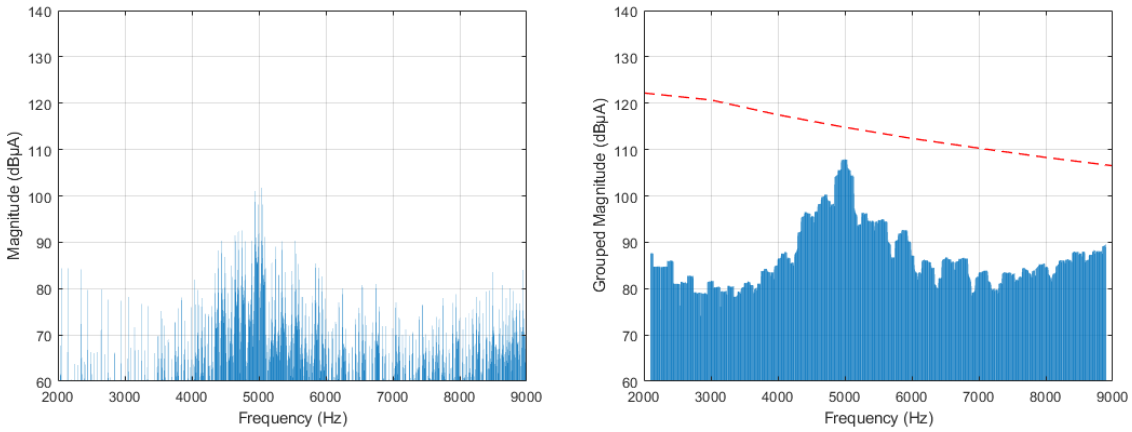

Figure 27: Simulated Drive A with the simpler cable model, current waveform (4.5 kHz, 510 rpm)

The simpler motor cable modeling reduced the simulation time from one hour to about 5 minutes, indicating that the model is significantly lighter. The values in Figure 27 are relatively similar as in Figure 23, which had the same operating point with the heavier cable model. Based on this, a simpler cable model using only capacitors to represent the cable characteristics would be sufficient for simulations in the 2-9 kHz range.

4.5 Conclusions for simulations

Simulations were performed for Drive A in a scenario where an unloaded 37 kW induction motor was operated at constant speed. The simulation was first conducted without modeling the motor cables and then with a 150 m motor cable model (16 mm^2 MCCMK). Without the cable model, the simulated emissions were unrealistically low. No significant magnitudes were observed at the frequencies corresponding to the switching frequency or its multiples in the spectrum. This increased the unreliability of the simulation model. However, the motor cable model provided promising indications that the simulation model could be useful for compliance testing once the accuracy of the simulation model is improved. Based on the existing simulation model, the harmonic emissions of Drive A remain below the limits in 2-

9 kHz range, while providing an indication that the length of the motor cable contributes to increasing emissions. However, the simulation model is not capable of accurately predicting harmonic emissions in the 2-9 kHz range, thus making it unsuitable for compliance testing purposes.

For future studies, it is advisable to include a motor cable modeling in the simulation model. To reduce the computational burden in simulations with cable modeling, it may be sufficient to use a simpler modeling approach for motor cable characterization by employing only capacitors, as shown in Figure 26.

For more in depth examinations, the simulation models could be improved by considering additional motor cable lengths and by investigating the causes of the software getting stuck during the simulations. No specific reason was found for the frequent freezing issues after modifying a parameter, such as the switching frequency. There were issues particularly with completing simulations when a load was added to the motor. Therefore, loaded motor simulations were excluded from the analysis.

It was suspected that the DLL file, that contains the inverter control source code, was causing the simulation model to become heavy, resulting in long simulation process and making it unstable and sensitive to parameter changes. One way to reduce the computational burden of the DLL file during the simulation could be by pre-storing the actual inverter switching data inside the model. This would facilitate the development of the simulation model.

5 Laboratory measurements against emission limits

In this chapter, the focus is on testing the selected VSDs against the emission limits proposed in the draft standard IEC 61000-3-10 through laboratory measurements. The basic information of the tested VSDs is listed in Appendix 1. The test setup included the AMN, which was presented in Section 3.7 Each VSD was tested in the speed control mode, without loading the motor, at switching frequencies of 1.5 kHz, 4.5 kHz and 12 kHz, operating with four different motor speeds: 150 rpm, 510 rpm, 1050 rpm and 1500 rpm. Under these operation points, the voltage and current waveforms were recorded. Each operation point was allowed to run for at least 10 seconds before the recording started. The results are presented in Sections 5.2 to 5.5

In addition, Drive B was tested in the torque control mode with a loaded motor. The purpose was to investigate the potential impact on harmonics in the 2-9 kHz frequency range under a loaded condition. The loaded motor tests are presented in Section 5.6

The evaluation process also includes reviewing the suitability of the EMI receiver and power analyzer for conducting these tests in accordance with the standard draft. The measurement data was primarily conducted with an oscilloscope, recording time domain waveforms of phase L1 current and L1-to-ground voltage. Data analysis, including FFT, was performed using MATLAB, similarly as with processing of the simulation data. The measurement equipment and test setup are discussed in Section 5.1

5.1 Testing facility and equipment

The EMC laboratory at ABB served as the primary test location. The laboratory is utilized for example in testing VSDs in accordance with the IEC 61800-3 standard. The laboratory is equipped with a 100 kVA transformer, which separates the test setups in the EMC laboratory from other nearby testing laboratories, ensuring minimized interference. The laboratory's supply network is of TN-S type, and its test area features a conductive metal floor used as the reference ground plane. Power for the test setup was sourced from a 32 A socket, with a nominal voltage of 400 V and a short circuit capacity of 5 kA.

As the laboratory's supply network is inherently loose, and to prevent disturbance caused by other test setups supplied by the same transformer, a Chroma 61512 programmable AC source was employed in the test setup, between the power supply and AMN. The output impedance of Chroma 61512 is very low, which adds extra stiffness to the system. The device was programmed to provide a non-distorted three-phase 230 V sine wave to the AMN.

In the measurement test setup for the unloaded motor, the AMN was grounded through the metallic floor. Additionally, the LISN was grounded on the input side through its power supply cable. The EUT was grounded separately to the floor. The motor was grounded to the EUT's chassis through the motor cable. The layout of the test setup used in the EMC laboratory is illustrated in Figure 28.

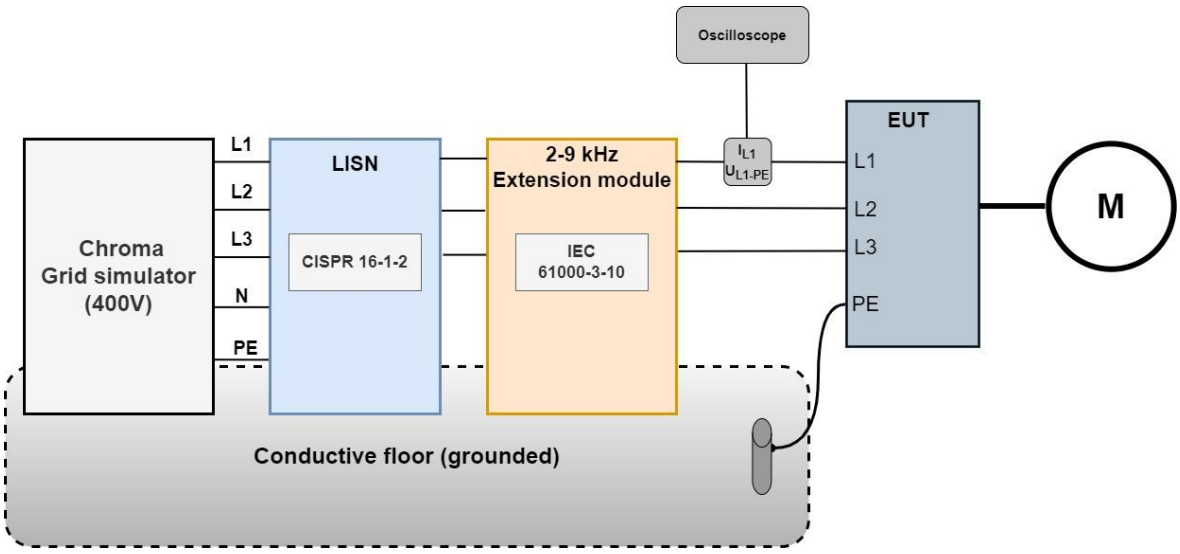

Figure 28: Layout of the test setup implemented in EMC laboratory

5.1.1 Tektronix MDO4104-3 oscilloscope

The Tektronix MDO4104-3 Oscilloscope was used as the primary measuring device during the measurements as it allowed for convenient recording of current and voltage waveforms.

The Tektronix TCP0150 current probe was used as the current measurement instrument for the oscilloscope. The probe current range was set to 25 A. The Pico Technology TA132 passive voltage probe was used in the voltage measurements. To prevent any voltage reaching the oscilloscope chassis via the passive probe, voltage measurement was taken between phase L1 and ground.

The oscilloscope was set to measure 250,000 samples per second. Voltage and current waveforms were recorded in a 400 ms time window. In MATLAB, a 200 ms window (10 periods) was clipped from the recorded data of 400 ms. The sampling frequency was also interpolated to 50 kHz, in order to calculate spectral components in 5 Hz intervals using FFT.

The data acquisition mode was set to the Hi Res mode to reduce the baseline noise. In Hi Res mode, the average of all samples is calculated for each acquisition interval, delivering a waveform with higher resolution and lower bandwidth (Tektronix 2012). Enabling the Hi Res mode had a noticeable impact, especially on the results of the voltage harmonic spectrum. Without this setting, the spectrum showed elevated voltage levels across the entire frequency range, leading to a relatively flat appearance after grouping. Consequently, it was challenging to distinguish the peaks corresponding to the inverter switching frequency within the background noise.

5.1.2 Yokogawa WT5000 power analyzer

In addition to the oscilloscope measurements, measurements were made with the WT5000 power analyzer to evaluate its suitability for performing harmonic measurements according to the IEC 61000-3-10. WT5000 is typically used for harmonic measurements in accordance with IEC 61800-3, where harmonics up to 2 kHz are considered. The wiring of the power analyzer was configured in a 3P4W connection, allowing direct voltage measurements to measure phase voltages. HITEC Zero-flux current transformers, rated for 1000A, were used as external current sensors for the power analyzer.

The device settings were configured as follows:

- Voltage range: 300 V
- Current range: 5 mA

- Line filter 30: kHz
- Frequency filter: 0.1 kHz

WT5000 included a separately purchased G7 option firmware, which enables automatic harmonic measurements according to IEC 61000-4-7 Edition 2.0 A1, incorporating harmonic and interharmonic grouping as illustrated in Figure 5. For recording the correct frequencies, the measurement range was set to cover the first 180 harmonics (up to 9 kHz), with a grouping type of "Type 2." As a result, the device displayed the first 180 voltage and current harmonic groups at 50 Hz intervals, having the surrounding interharmonics included in the groups as according to the IEC 61000-4-7 standard.

In the IEC Harmonics mode, a practical issue was the difficulty of exporting measurement data from the device. Normal data storing functions (e.g. using a USB memory stick) were blocked when using the IEC Harmonic Mode, as confirmed by a local Yokogawa representative (Haapamäki 2022). According to instructions sent from Yokogawa, a PC program called DL-Terminal had to be used, which would retrieve the measurement data of an individual measurement point from the power analyzer and print it in the ASCII text mode within the program window. The measurement data, consisting of the magnitudes of 180 voltage and current harmonic groups, was manually transferred into an Excel file. Additionally, the corresponding frequency for each harmonic group was added to ensure compatibility with a simple MATLAB code for data interpretation.

One challenge in using the WT5000 was that the IEC61000-3-10 compliant grouping was not possible because the raw data was recorded at 50 Hz intervals instead of 5 Hz intervals. As a result, post-processing grouping, as done with the oscilloscope data, was not feasible. However, the WT5000 firmware accounted for interharmonics through its Type 2 grouping, so the measurement results provided by the device were close to the results obtained from the oscilloscope. Another challenge with the WT5000 was the time-consuming process of manually exporting the measurement data from the device to MATLAB using DL-Terminal and Excel.

On the positive side, the WT5000 was capable of simultaneously measuring currents and voltages of all phases, making it well-suited for studying harmonics in frequency converters within the 2-9 kHz range. However, due to the grouping issue, the device did not fully meet the requirements for official compliance measurements. It is expected that when IEC 61000-

3-10 officially comes into effect, measurement device manufacturers will likely release software add-ons, which would allow user-friendly automatic measurement of harmonics and interharmonics according to the standard, including the necessary grouping.

5.1.3 Rohde & Schwartz ESW EMI test receiver ESW8

Another measurement device that was included in the evaluations was the Rohde & Schwarz ESW EMI test receiver ESW8, which has a frequency range of 1 Hz to 8 GHz. This device is typically used in EMC laboratories for conducting Conductive EMI measurements of frequency converters, particularly in the range of 150 kHz to 30 MHz. Due to its application in EMI measurements, testing the device drew interest.

For the 2-9 kHz measurements with the ESW8, an external R&S EZ-17 current probe with a frequency range of 20 Hz to 100 MHz was used. Typically, in EMI measurements, the EMI receiver measures directly from the LISN through a coaxial cable. However, in this work, the measurement location was between the frequency extension module prototype and the EUT. The current was measured from the phase L1 cable.

Only the current of one phase could be measured at a time, and there was no measurement capability for voltage. However, the voltage measurement would not have been necessary since the AMN was implemented in the test setup, as stated in the standard draft.

The ESW8 required configuration of correction factors for the current probe, which were set according to the probe’s calibration certificate. The correction factors adjust for the probe's frequency response and ensure accurate measurements within the 2-9 kHz frequency range. In addition, the limit line for currents, calculated in section 3.3, was manually set on the device's display for visual reference.

With the ESW8, measurement data from an individual measurement point could be quickly displayed as a waveform on the device's screen, allowing for immediate comparison with the limit line. The measurement data could also be easily saved to a USB stick in CSV format. However, the ESW8 faced a similar issue as the WT5000 as attempts to adjust the settings failed in enabling the device to measure at 5 Hz intervals. The measurement capability of the ESW8 was limited to 50 Hz intervals, and there were no indications in the menus or manual regarding the grouping spectral components.

5.2 Drive A

Drive A is a 37 kW VSD, that contains a 6-pulse rectifier and an internal DC choke in its DC-link. For the measurements, a 37-kW induction motor and a 5 m long 16 mm^2 MCCMK motor cable were used. The VSD was also tested with a 150 m long motor cable.

Drive A was operating at switching frequencies of 1.5 kHz, 4.5 kHz and 12 kHz, with four different motor speeds: 150 rpm, 510 rpm, 1050 rpm and 1500 rpm. While using these switching frequencies and motor speeds, the voltage and current waveforms were recorded with the oscilloscope.

5.2.1 Tests with a 5 m motor cable

Figure 29 shows the waveforms in time domain when Drive A with a 5 m motor cable was operating at 4.5 kHz and 510 rpm. The measured current waveform contains more distortion than the simulated waveform of current (Figure 15), while also having slightly higher peaks.

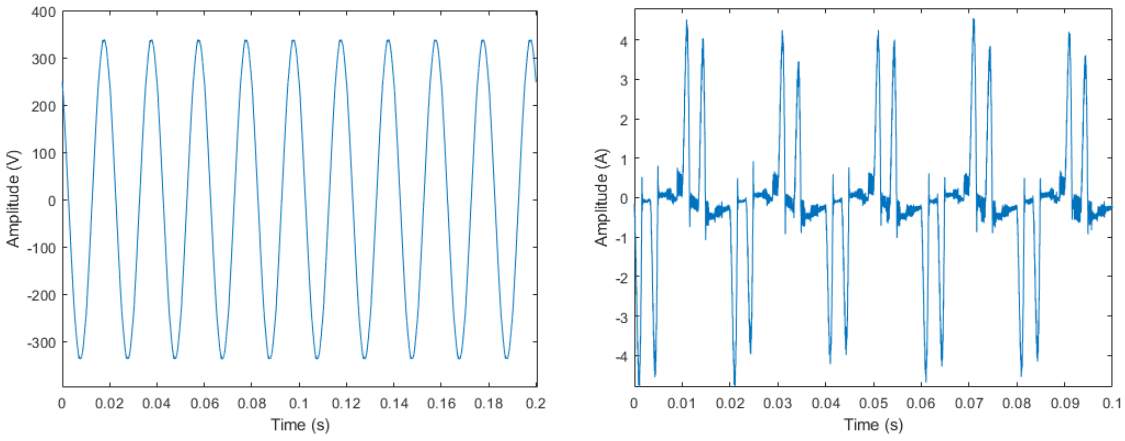

Figure 29: Drive A, voltage and current waveforms in time domain (4.5 kHz, 510 rpm)

Figure 30 and Figure 31 show the voltage and current in the frequency domain. The diagrams were generated in a similar manner to the simulation diagrams, using FFT analysis and converting the values to dBµV and dBµA units in MATLAB. The right-hand diagrams have

utilized the grouping method specified in the draft standard, allowing for a comparison of the results with the red dashed line, which represents the limits calculated in Section 3.3

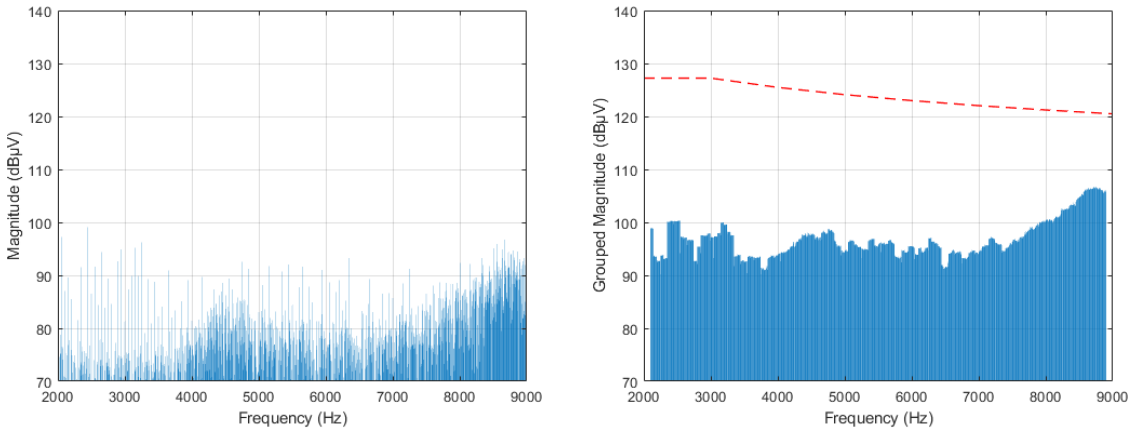

Figure 30: Drive A, voltage waveform in frequency domain (4.5 kHz, 510 rpm)

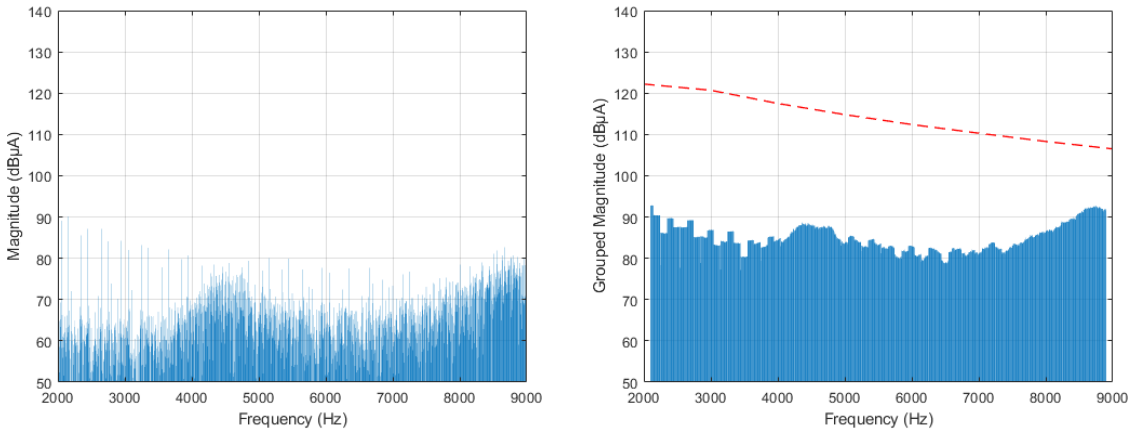

Figure 31: Drive A, current waveform in frequency domain (4.5 kHz, 510 rpm)

The same operating point was also measured using ESW8 and WT5000. The results can be seen in Figure 32. When comparing the ESW8 and WT5000 measurements to oscilloscope measurements, the small differences in magnitudes can mostly be attributed to the different grouping methods employed by the devices' software, which did not use the grouping method described in the standard draft.

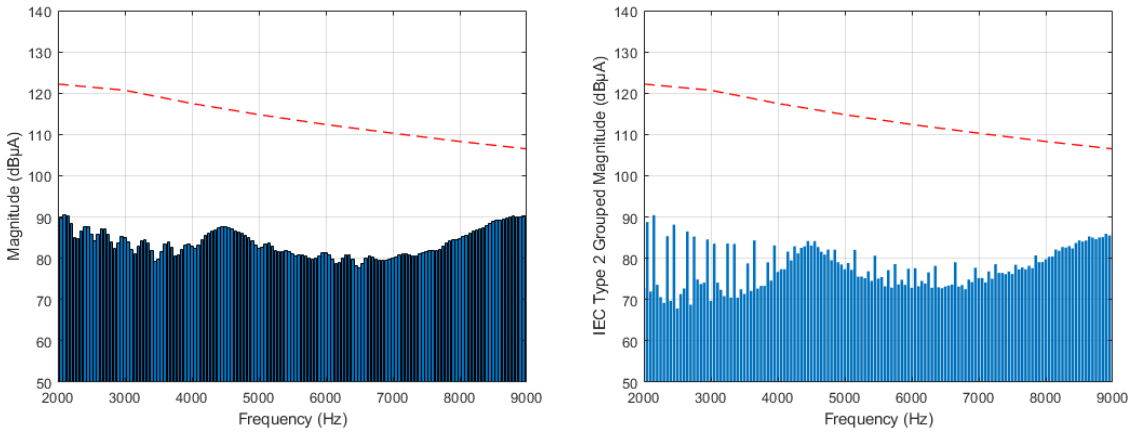

Figure 32: Drive A, ESW8 and WT5000 measurements (4.5 kHz, 510 rpm)

Figure 30 and Figure 31 show that the voltage and current harmonic emissions stay under the limits in the 2-9 kHz range. ESW8 and WT5000 are showing similar results, as shown in Figure 32. Higher magnitudes can be observed around the frequency corresponding to the switching frequency (at 4.5 kHz) and double the switching frequency (9 kHz).

Measurements for Drive A with a 5 m long motor cable show that the emissions are well under the limits in the 2-9 kHz range, with 1.5 kHz, 4.5 kHz and 12 kHz switching frequencies. Figure 33 shows the emissions in grouped dBµA values of all motor speeds with a 4.5 kHz switching frequency.

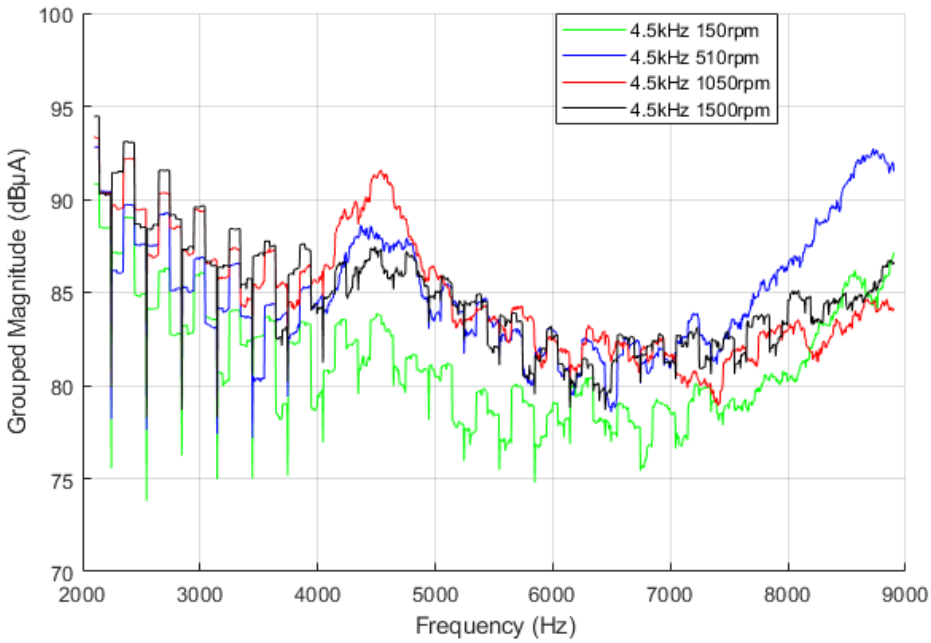

Figure 33: Drive A with 5 m cable, grouped current waveforms in frequency domain, (4.5 kHz, all motor speeds)

It can be observed that the highest values are measured in the lower end of the frequency range with 1500 rpm. Near the frequency corresponding to the switching frequency, the highest emissions are measured with 1050 rpm. However, near the upper end of the frequency range the highest values are measured with 510 rpm. In general, the lowest emissions are measured with 150 rpm.

Similar phenomena as with the 4.5 kHz switching frequency did not occur with switching frequencies of 1.5 kHz and 12 kHz, in the 2-9 kHz range, as can be observed from Figure 34.

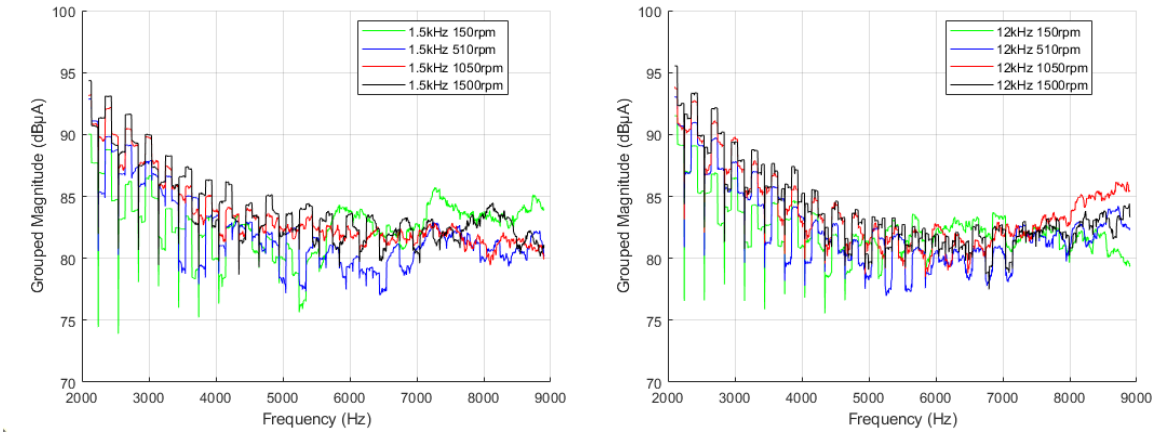

Figure 34: Drive A, with 5 m cable, grouped current waveforms in frequency domain, (1.5 and 12 kHz, all motor speeds)

Similarities with the 4.5 kHz switching frequency are found only in the lower end of the frequency range. Higher values were measured outside the frequency range. For example, with a switching frequency of 12 kHz, higher values appeared near the 12 kHz frequency. This indicates that higher peaks in the 2-9 kHz range can be expected only with switching frequencies of 2-9 kHz.

5.2.2 Tests with a 150 m motor cable

The 5 m long motor cable was replaced with a 150 m long motor cable (16 mm^2 MCCMK) and the measurements were repeated for the 4.5 kHz switching frequency. Figure 35 shows the voltage and current waveforms in time domain for a 4.5 kHz switching frequency and 510 rpm motor speed, while employing the 150 m long motor cable.

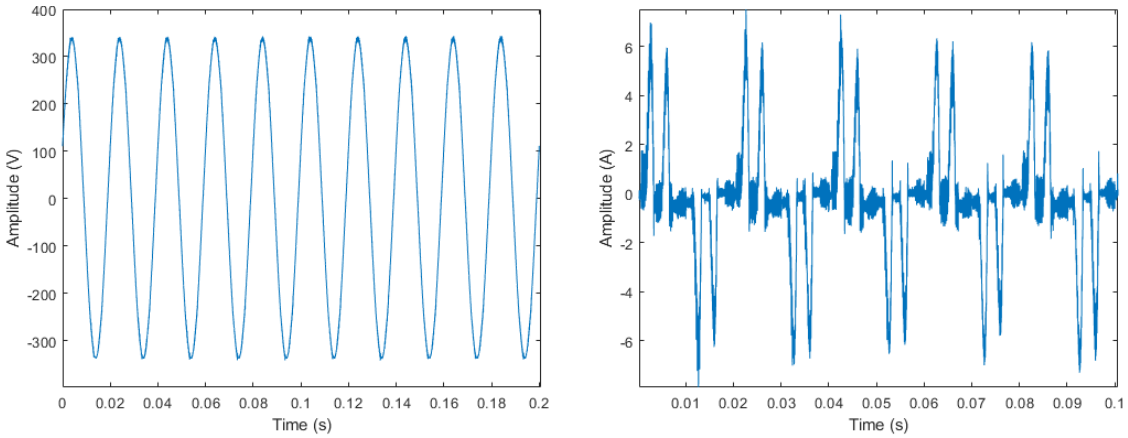

Figure 35: Drive A with 150 m cable, voltage and current waveforms in time domain (4.5 kHz, 510 rpm)

The effect of the longer motor cable is presented in Figure 36, where the left-hand waveform shows the previous measurement with 5 m motor cable, while the right-hand waveform shows the result with the 150 m cable. The result shows increased distortion in the current waveform when the 150 m motor cable is used.

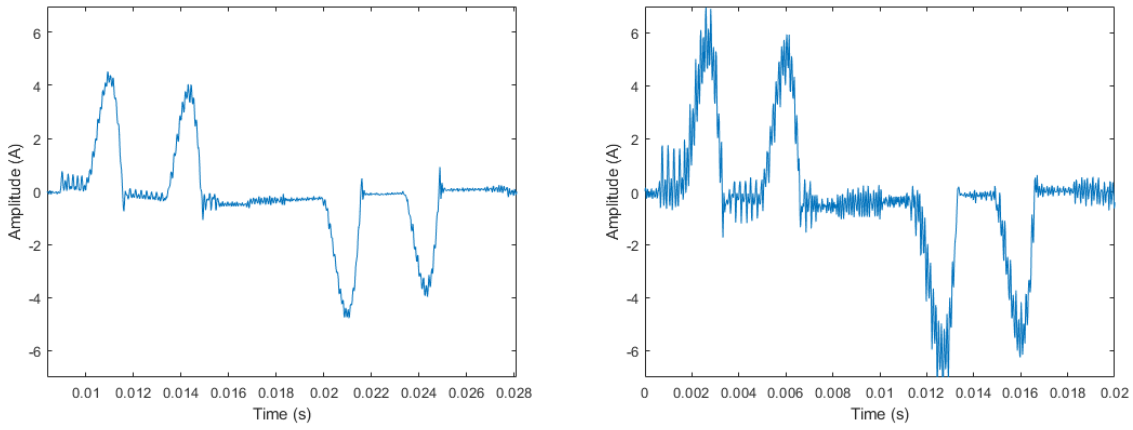

Figure 36: Drive A current waveforms in time domain, 5 m vs 150 m motor cable comparison (4.5 kHz, 510 rpm)

Figure 37 and Figure 38 present the voltage and current waveforms in frequency domain, showing higher magnitudes around 4.5 kHz and 9 kHz. The change is significant at the end of the frequency range, as there were already higher magnitudes in that region. As a result,

both the current and voltage values approach the emission limit, as can be seen in the right-hand side diagrams. The difference from the highest point to the limit line is approximately 2.9 dBµV for the voltage and 3.1 dBµA for the current.

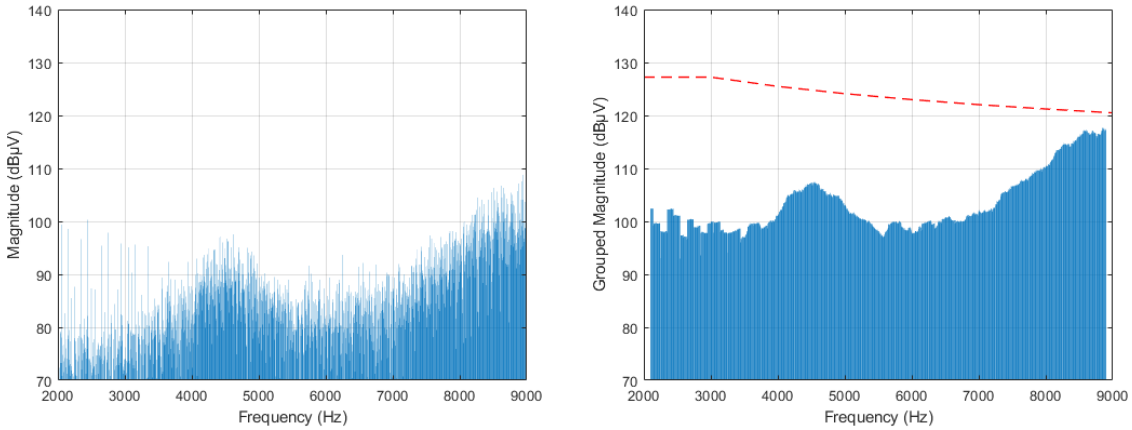

Figure 37: Drive A with 150 m cable, voltage waveform in frequency domain (4.5 kHz, 510 rpm)

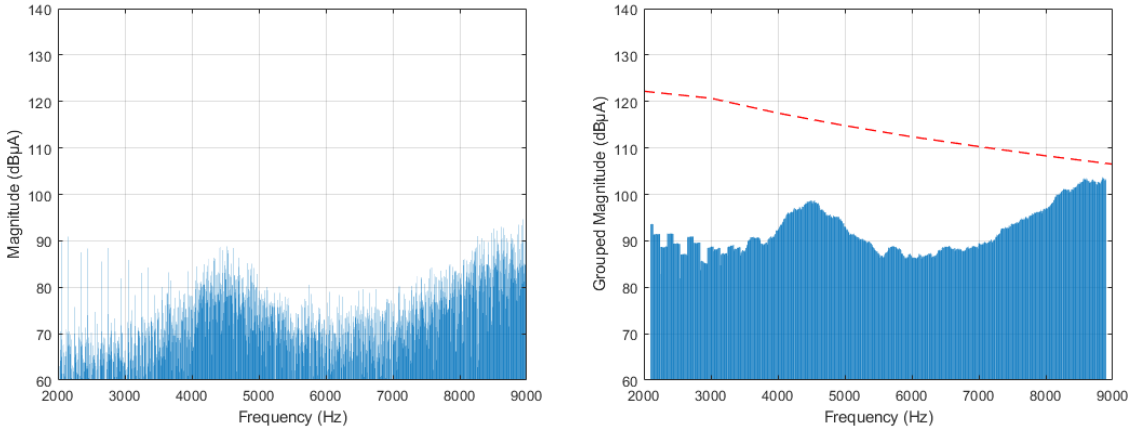

Figure 38: Drive A with 150 m cable, current waveform in frequency domain (4.5 kHz, 510 rpm)

Figure 39 illustrates the frequency domain waveforms of Drive A, with both short and long cables, at all tested rotational speeds. The solid lines represent the results with a 5 m cable, while the dashed lines represent the results with a 150 m cable. It is observed that replacing the 5 m long motor cable with a 150 m long cable clearly has an effect on the harmonic

emissions of Drive A. The effect is visible approximately from 3.5 kHz and higher frequencies. Using the longer cable resulted in an increase of current magnitudes (grouped) from 5 to 10 dBµA.

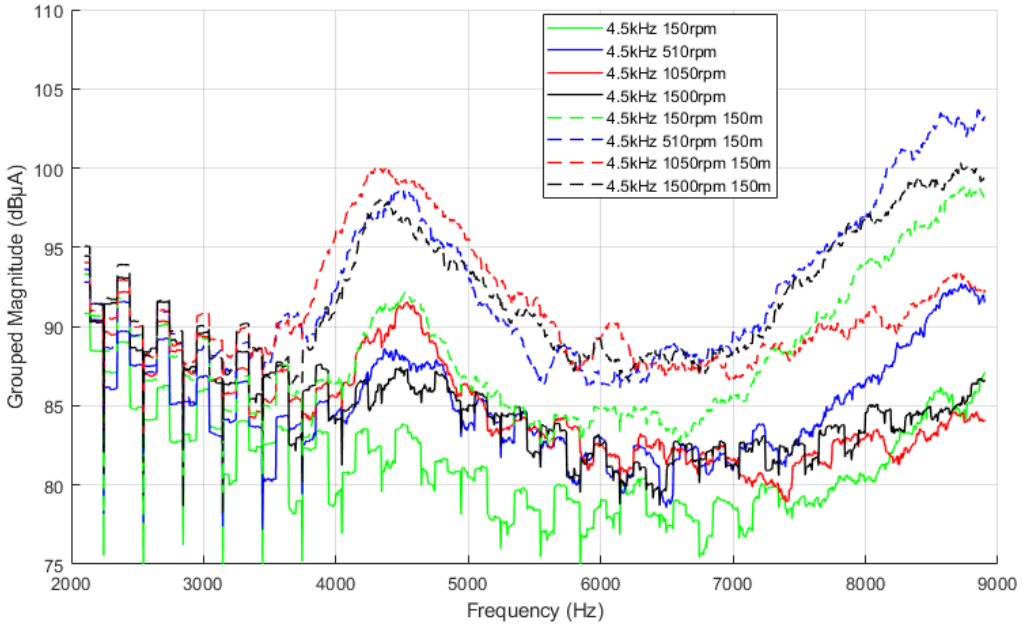

Figure 39: Drive A, all current waveforms in frequency domain for 4.5 kHz (5 m and 150 m cables)

Measurements for Drive A with the 150 m long motor cable show that harmonic emissions in the 2-9 kHz frequency range remain below the specified limits. Although using a longer cable resulted in higher emissions at all motor speeds, the emissions still remained within the limits defined by the standard draft. The highest current emissions were observed at the higher end of the frequency range, with 510 rpm motor speed (approximately 103.7 dBµA).

A possible reason for increased emissions with the longer cable is the presence of stray capacitances of the cable. The cable capacitances are directly proportional to the length of the cable. When the inverter's IGBTs switch rapidly, the cable capacitances will be charged and discharged in sync with the switching operations. This, in turn, leads to additional current spikes in the inverter.

5.3 Drive B

Drive B is a smaller version of Drive A, having a nominal power of 1.1 kW. It contains a 6-pulse diode rectifier and an internal DC choke. For the measurements, a 1.5 kW induction motor and a 5 m long 2.5 mm^2 MCCMK motor cable were used. Measured operating points (switching frequencies and motor speeds) were the same as with Drive A.

Figure 40 shows the voltage and current waveforms in the time domain when Drive B was operating at 4.5 kHz and 510 rpm. The small power of Drive B is clearly visible in the current waveform.

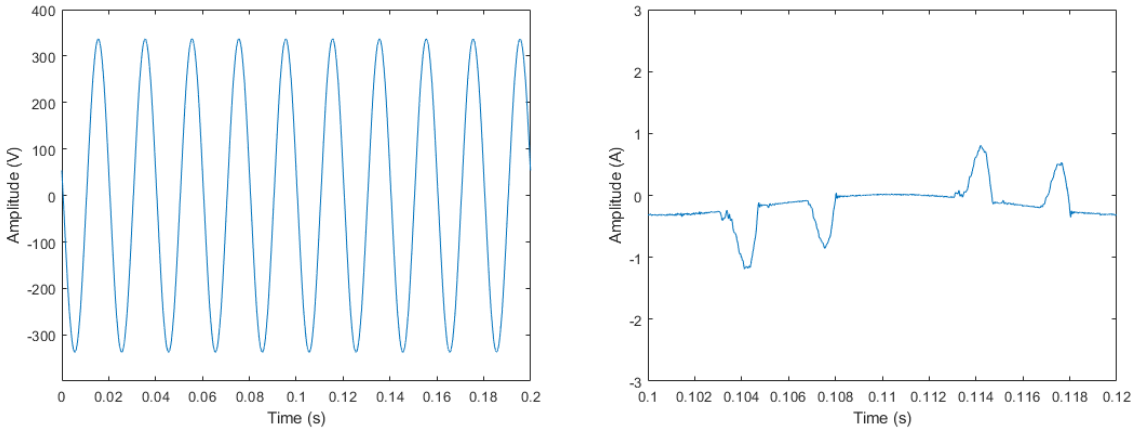

Figure 40: Drive B, voltage and current waveforms in time domain (4.5 kHz, 510 rpm)

Figure 41 and Figure 42 show the voltage and current waveforms in the frequency domain. For voltage, there are no distinct peaks at 4.5 kHz or 9 kHz because there are relatively high magnitudes across the entire frequency range. In contrast, the current spectrum clearly shows peaks near 4.5 kHz and 9 kHz.

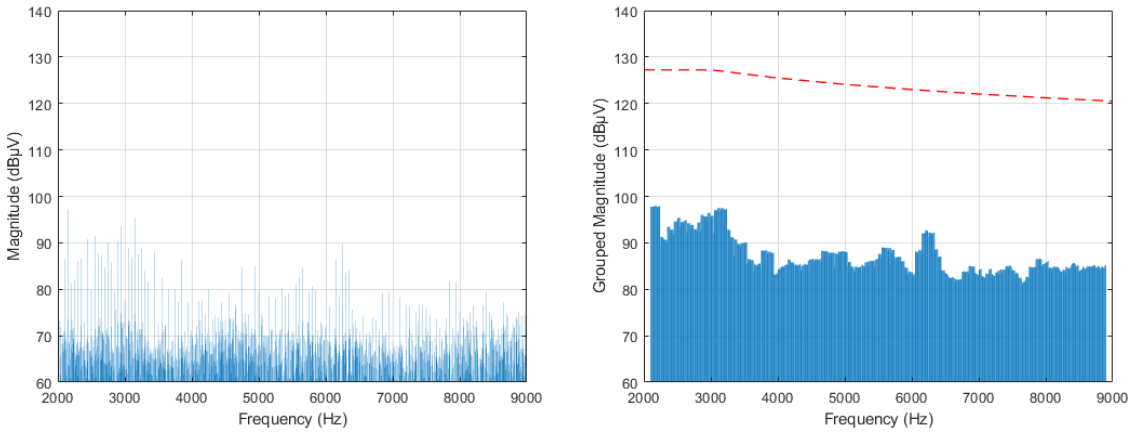

Figure 41: Drive B, voltage waveform in frequency domain (4.5 kHz, 510 rpm)

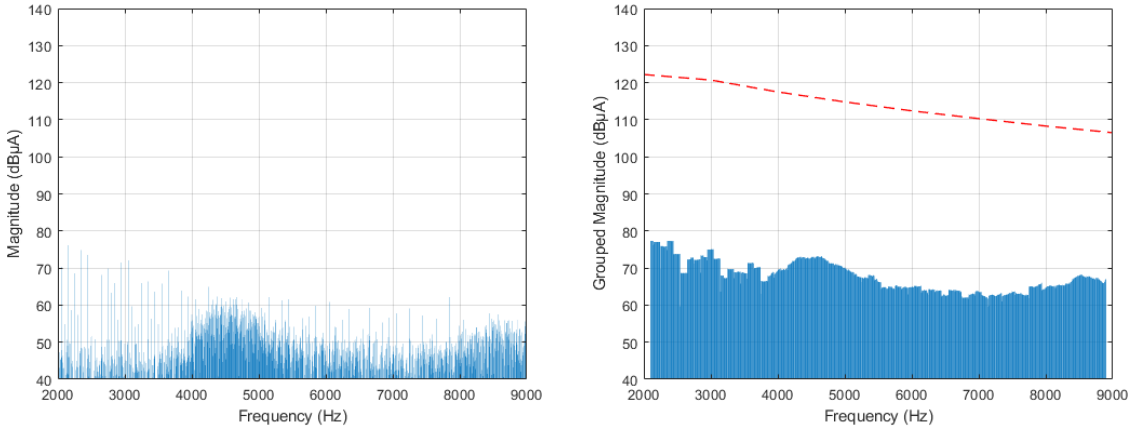

Figure 42: Drive B, current waveform in frequency domain (4.5 kHz, 510 rpm)

Compared to Drive A with a 5 m motor cable (Figure 31), the current magnitudes are approximately 15-20 dBµA lower for Drive B at 4.5 kHz and 9 kHz. Based on the measurements, it can be concluded that the harmonic emissions of Drive B in the 2-9 kHz range are overall far below the limits defined by the draft standard.

5.4 Drive C

Drive C is an AFE or a four-quadrant VSD that contains a line-side converter and a motor-side converter. Both converters compose of six IGBTs. Additionally, there is an LCL filter on the supply side that provides suppression of the harmonics. The VSD is known as a low harmonic drive, particularly when considering harmonics below 2 kHz. Typically, higher

frequency harmonics (above 2 kHz) have been more problematic, as they tend to increase with this type of drive.

The rated nominal power of Drive C is 37 kW. It was tested using the same 5 m cable and 37 kW motor as Drive A. In addition, Drive C was tested with a 100 m cable length, because the VSD's specified maximum cable length is 100 m to comply with category C2 of the IEC 61800-3 standard. Similar to the previously tested drives, the voltage and current harmonics of Drive C were recorded using the oscilloscope and FFT analysis in MATLAB. The measurements were taken at the same switching frequencies and motor speeds as the previously tested drives.

5.4.1 Tests with a 5 m motor cable

Figure 43 shows the voltage and current waveforms in the time domain when Drive C was operating at 4.5 kHz and 510 rpm. The figure shows that the current waveform of the AFE drive is more sinusoidal than for a drive with a diode rectifier.

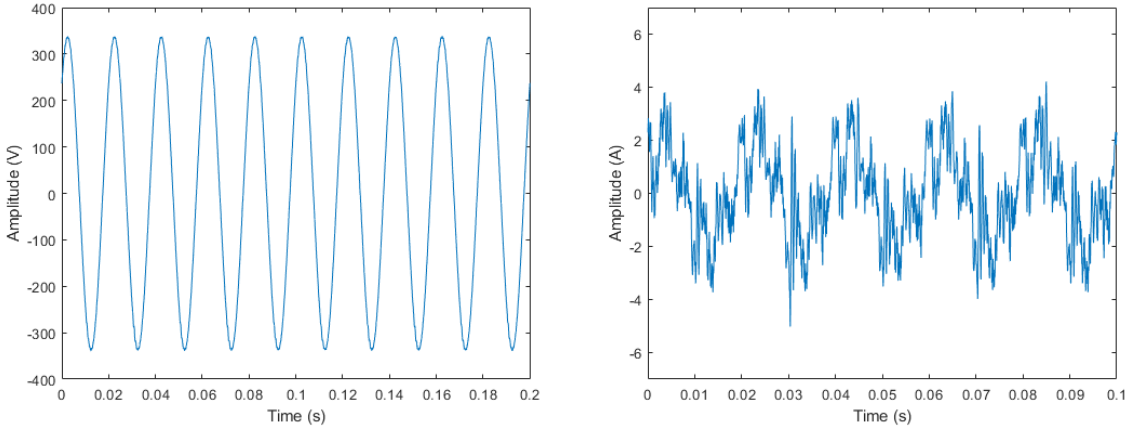

Figure 43: Drive C with 5 m cable, voltage and current waveforms in time domain (4.5 kHz, 510 rpm)

Figure 44 and Figure 45 show the voltage and current waveforms in the frequency domain with a 4.5 switching frequency and 510 rpm. Higher values occur at a frequency corresponding to the switching frequency, as with previously tested drives. The diagrams also reveal significantly elevated values near 6 kHz, which are due to the presence of the

IGBT rectifier. The difference from the highest point to the limit line is approximately 7.9 dBµV for the voltage and 8.7 dBµA for the current.

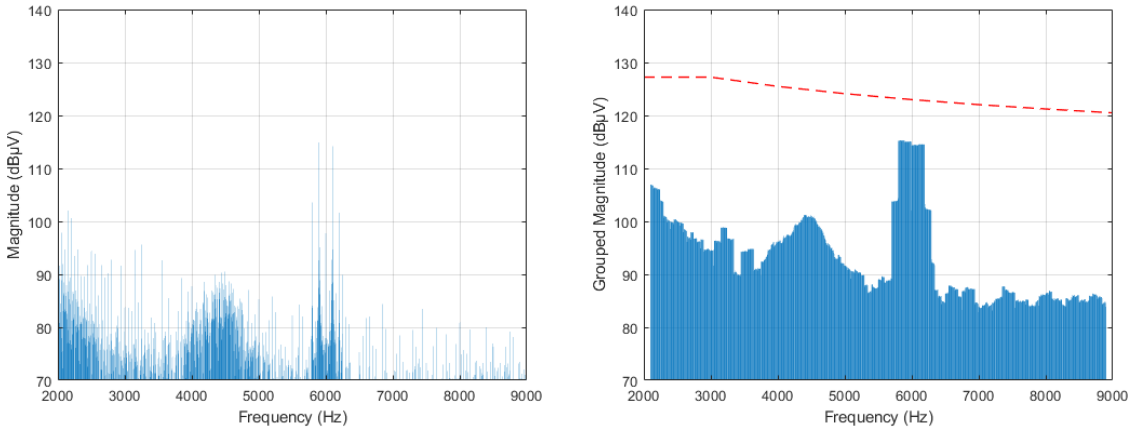

Figure 44: Drive C with 5 m cable, voltage waveform in frequency domain (4.5 kHz, 510 rpm)

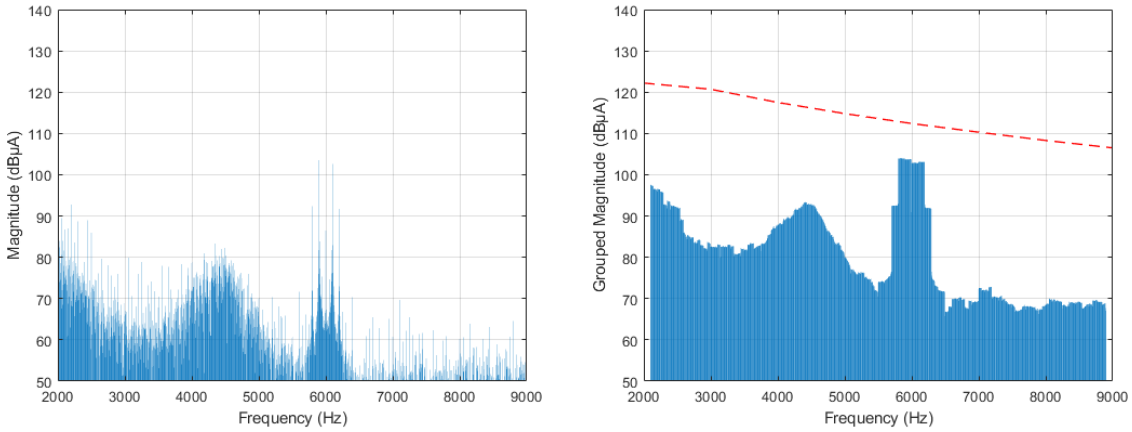

Figure 45: Drive C with 5 m cable, current waveform in frequency domain (4.5 kHz, 510 rpm)

Compared to the corresponding results of Drive A, which has a diode rectifier (Figure 30 and 31), the spectrum of Drive C shows low values at the higher end of the frequency range (7.5-9 kHz), where Drive A had shown significant peaks at that frequency range. Conversely, Drive C has significantly higher values at the lower end of the frequency range.

5.4.2 Tests with a 100 m motor cable

The 5 m motor cable was replaced with a 100 m motor cable, and the measurements were repeated for a 4.5 kHz switching frequency. Figure 46 shows the voltage and current waveforms in time domain when Drive C was operating at 4.5 kHz and 510 rpm. The waveforms are similar to those seen with a 5-meter cable.

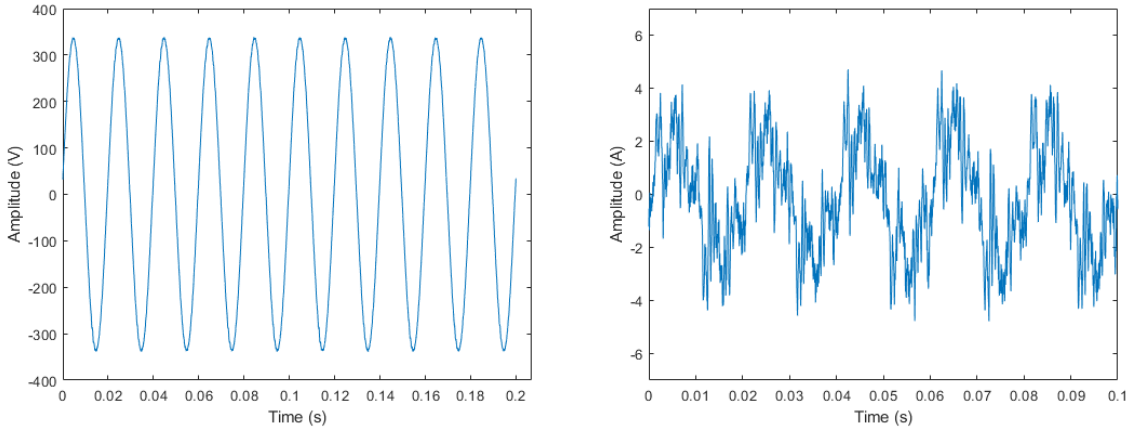

Figure 46: Drive C with 100 m cable, voltage and current waveforms in time domain (4.5 kHz, 510 rpm)

The voltage and current waveforms in the frequency domain are shown in Figure 47 and Figure 48. The diagrams indicate that there is no increase in emissions at 6 kHz when using a longer motor cable. While emissions slightly increase in other frequency ranges, it is not critical for Drive C from the perspective of emission limits.

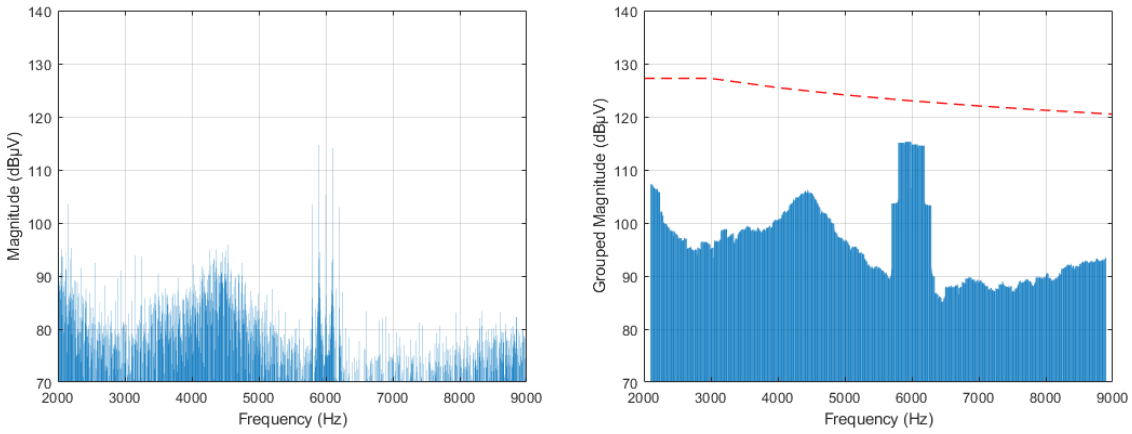

Figure 47: Drive C with 100 m cable, voltage waveform in frequency domain (4.5 kHz, 510 rpm)

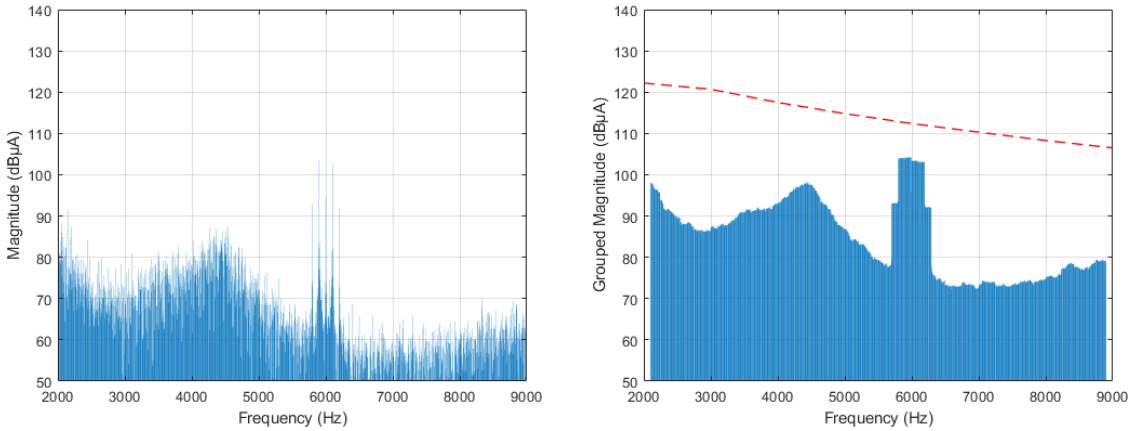

Figure 48: Drive C with 100 m cable, current waveform in frequency domain (4.5 kHz, 510 rpm)

Figure 49 displays all measured current waveforms of Drive C in the frequency domain, showing the comparison between the short and long cables. The graphs show that the peaks in the vicinity of 6 kHz are similar for both the 5 m and 100 m motor cables. In other frequency areas, emissions are about 3-10 dBµA higher for the longer cable.

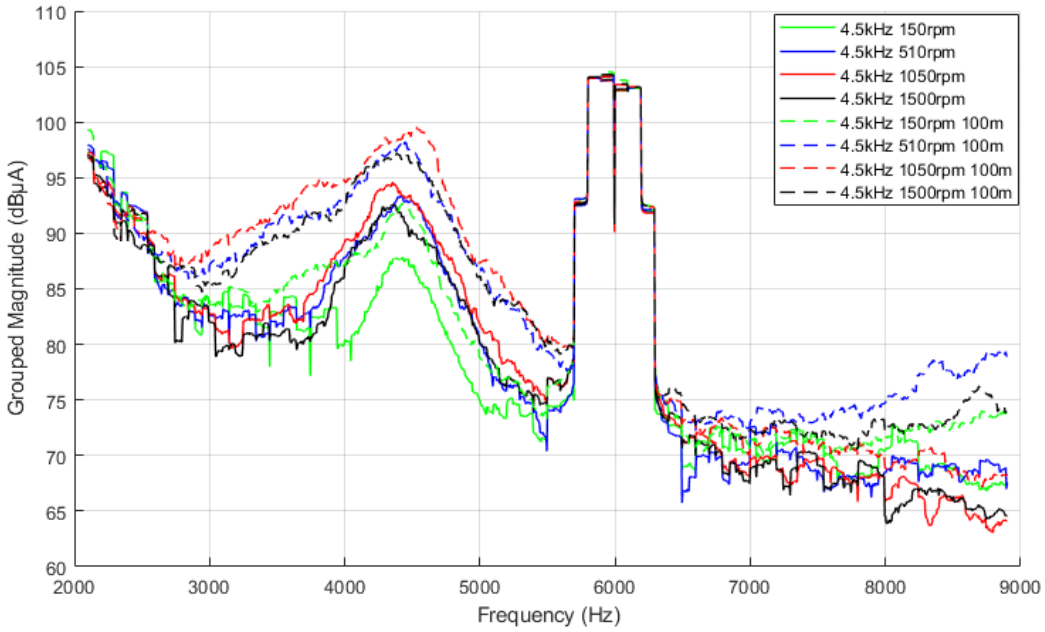

Figure 49: Drive C current waveforms in frequency domain, all motor speeds, 5 m cable vs 100 m cable

The measurement results for Drive C show that the device's harmonic emissions do not exceed the limits set in the standard draft. The measurements revealed peaks around 6 kHz, which are caused by the operation of IGBT rectifier. It is observed that using the longer cable did not affect emissions around the 6 kHz area. Results also indicate that the LCL filter on the input side is effective in filtering emissions in the 2-9 kHz range.

5.5 Drive D

Drive D is a 22 kW VSD that is optimized for machinery applications. It has a 6-pulse diode rectifier similar to Drive A or B, but it does not have an internal DC-choke. For filtering out disturbances, an external 0.45 mH AC-reactor is specified for Drive D. Measurements were conducted at 4 kHz, both without the external AC-reactor and with it.

5.5.1 Without external AC choke

Figure 50 shows the waveforms in the time domain when Drive D was operating at 510 rpm, showing similar waveforms as the other tested VSDs with diode rectifiers.

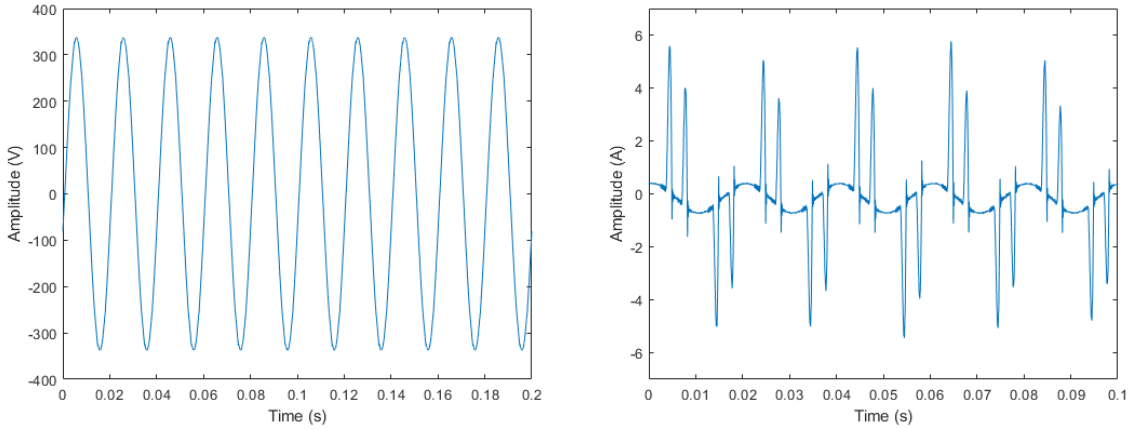

Figure 50: Drive D without AC-reactor, voltage and current waveforms in time domain (4 kHz, 510 rpm)

Figure 51 and Figure 52 show the waveforms of voltage and current in frequency domain. It can be observed that they exhibit a relatively flat profile, indicating that emissions resulting from the switching frequency are not clearly distinguishable at 4 or 8 kHz. The measurements, however, indicate that even without the external AC reactor, the emissions from Drive D are around 20-30 dBµV or dBµA below the limit lines.

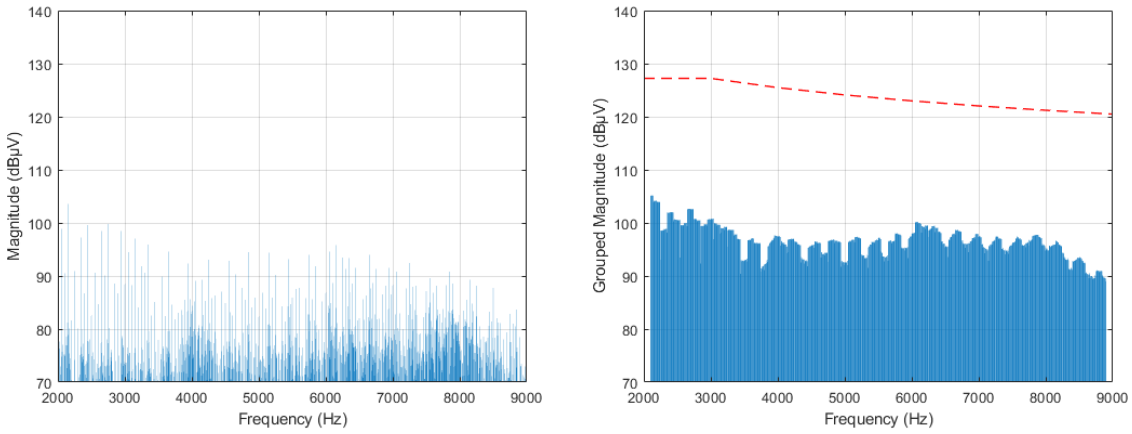

Figure 51: Drive D without AC-reactor, voltage waveform in frequency domain, (4 kHz, 510 rpm)

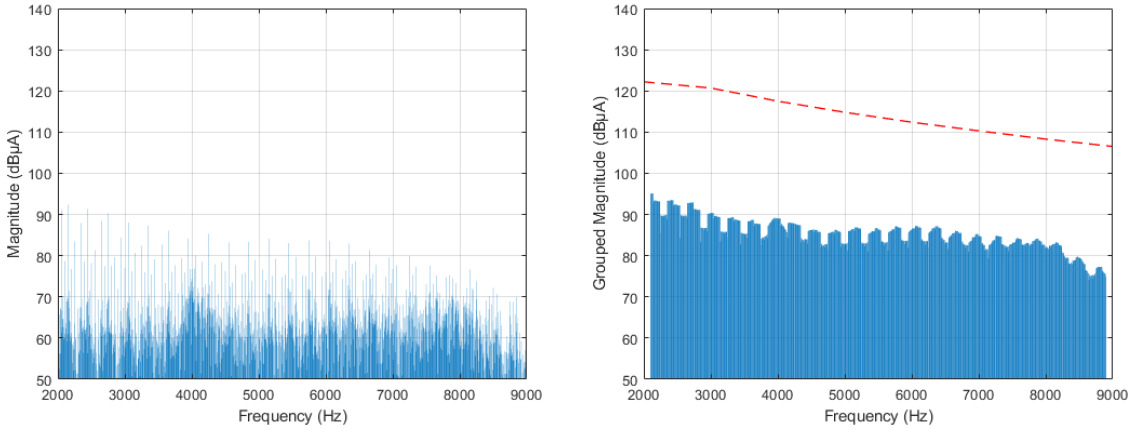

Figure 52: Drive D without AC-reactor, current waveform in frequency domain, (4 kHz, 510 rpm)

5.5.2 With external AC choke

The external AC reactor was installed between Drive D and the AMN, and the measurements were repeated. Figure 53 shows the waveforms in time domain when Drive D was operating at 510 rpm, showing slightly lower current spikes.

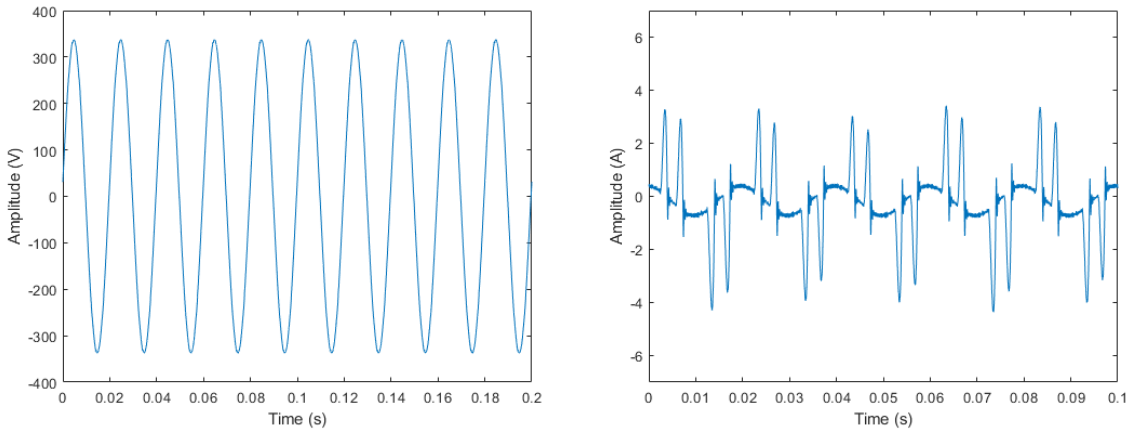

Figure 53: Drive D with AC-reactor, voltage and current waveforms in time domain (4 kHz, 510 rpm)

Figure 54 and Figure 55 show the waveforms of voltage and current in the frequency domain. It can be observed that the values are lower for Drive D with the external AC reactor. The emissions resulting from the switching frequency are more distinguishable at 4 and 8 kHz, because the background noise is lower. There are also voltage peaks above and below 6 kHz.

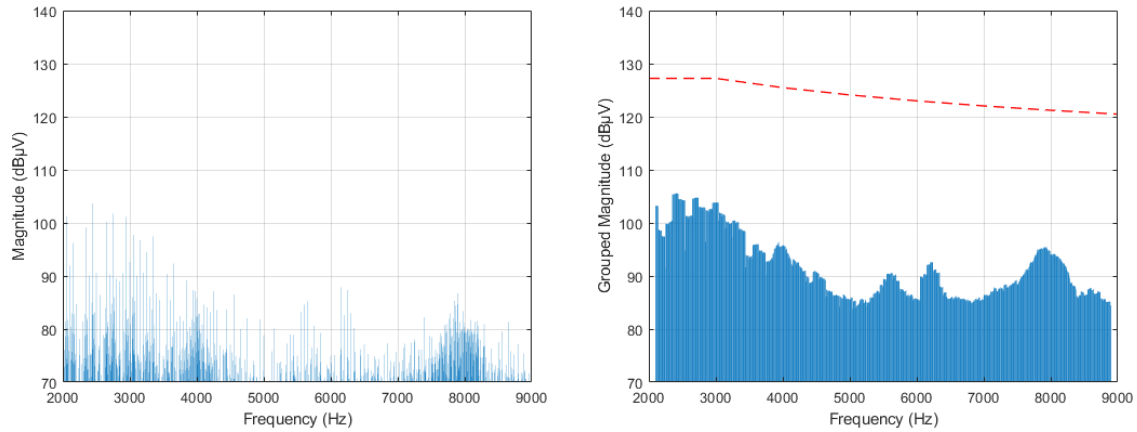

Figure 54: Drive D with AC-reactor, voltage waveforms in frequency domain (4 kHz, 510 rpm)

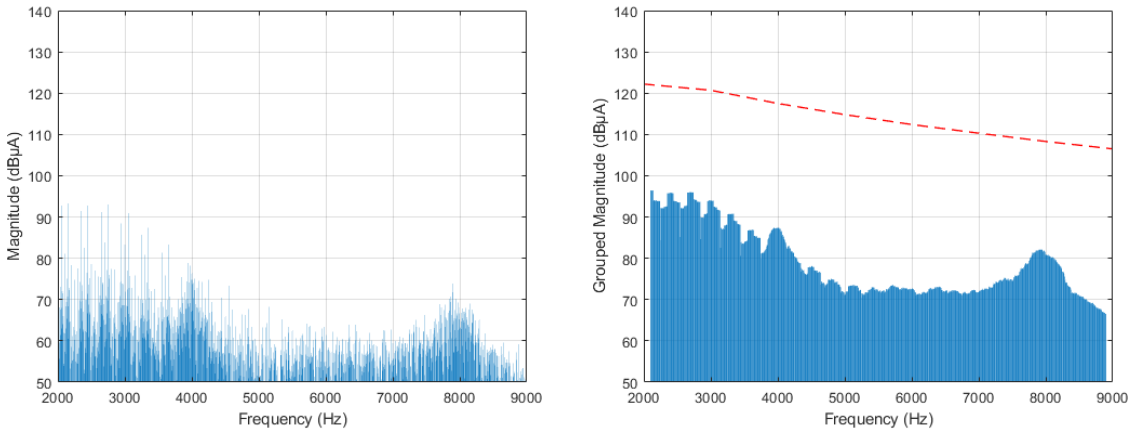

Figure 55: Drive D with AC-reactor, current waveforms in frequency domain (4 kHz, 510 rpm)

In Figure 56, the graphs of all operating points for Drive D at 4 kHz are compiled, demonstrating the impact of the AC-reactor on current emissions in the 2-9 kHz range. Measurements without the AC-reactor are represented by dashed lines, while solid lines indicate the corresponding points that have the AC-reactor installed.

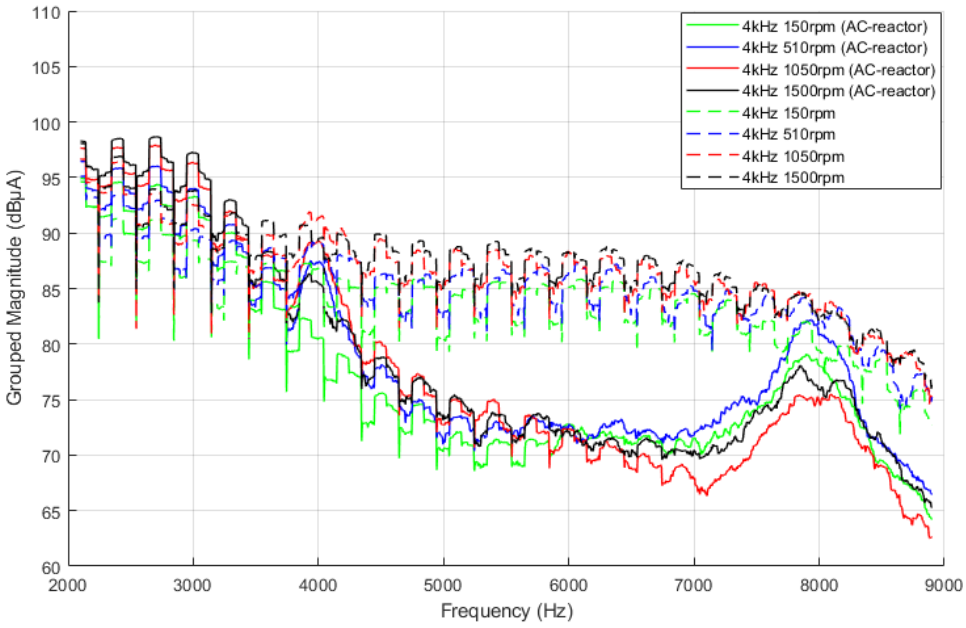

Figure 56: Drive D, the impact of the external AC-reactor on current emissions

The largest differences are observed in the range between 4 kHz and 8 kHz, where the AC-reactor yields up to 15 dBµA lower values. The variation in motor speeds did not have a significant impact in either case. Based on the measurements, the emissions of Drive D are clearly below the threshold in the 2-9 kHz range.

5.6 Drive B under load conditions

The harmonics of Drive B were also measured in a common laboratory, where it was possible to use a test setup with motor loads. Since the maximum current for the AMN was 16 A, Drive B was the most sensible option to be tested with a loaded motor. The anticipated outcome was that the harmonic emissions in the 2-9 kHz range would not increase considerably under load conditions.

The laboratory operated as an IT system, also known as a floating network. In order to conduct tests with the AMN, which had a ground leakage of 10A, an isolation transformer had to be used in the test setup. The motor used was a 2.2 kW induction motor, with a 4 kW load machine connected to it. The motor and load machine were located in the nearby hall. The length of the motor cables was estimated to be approximately 30 meters. As in the previous tests, a Chroma grid simulator, located in the nearby hall, was utilized as a supply in the test setup, providing extra stiffness to the system. Since the laboratory did not have a similar metal floor for a reference ground, the isolation transformer, AMN, and EUT were grounded to a grounding bus via conductors. The measurement equipment used was the same as in the unloaded tests, including the oscilloscope, current probe, and voltage probe. The overall structure of the test setup with loaded motor is presented in Figure 57.

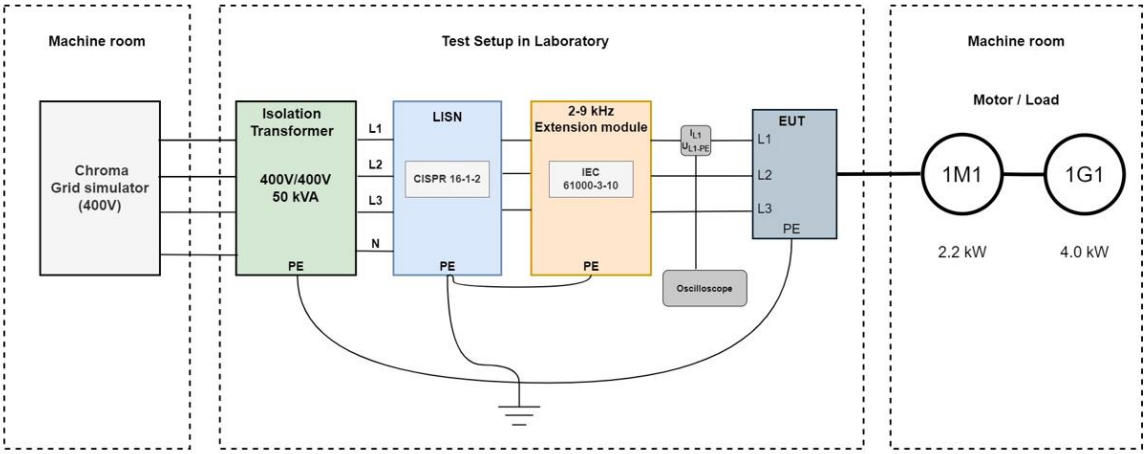

Figure 57: Laboratory test setup for loaded motor

Drive B was tested in the torque control mode at speeds of 150, 510, 1050, and 1500 rpm with motor currents of 1.0 A, 1.65 A, 2.5 A, and 3.3 A. 3.3 A is the rated nominal output current of Drive B. The measurements were taken with switching frequency of 4.5 kHz only. As an example, the voltage and current waveforms of the operating point at 510 rpm speed and 3.3 A motor current are shown in the time domain in Figure 58.

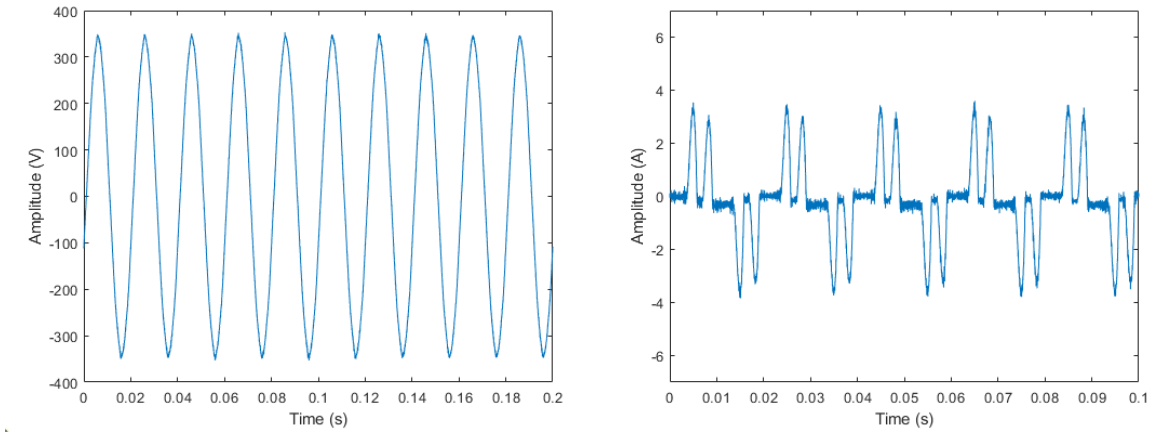

Figure 58: Drive B with loaded motor, voltage and current waveforms in time domain (4.5 kHz, 510 rpm, 3.3 A)

Voltage waveforms in the frequency domain are presented in Figure 59. Based on the diagrams, there is background noise in the voltage measurement that makes certain voltage

harmonics undistinguishable. This was the case for all operating points. However, the measured values are still relatively far from the limit line.

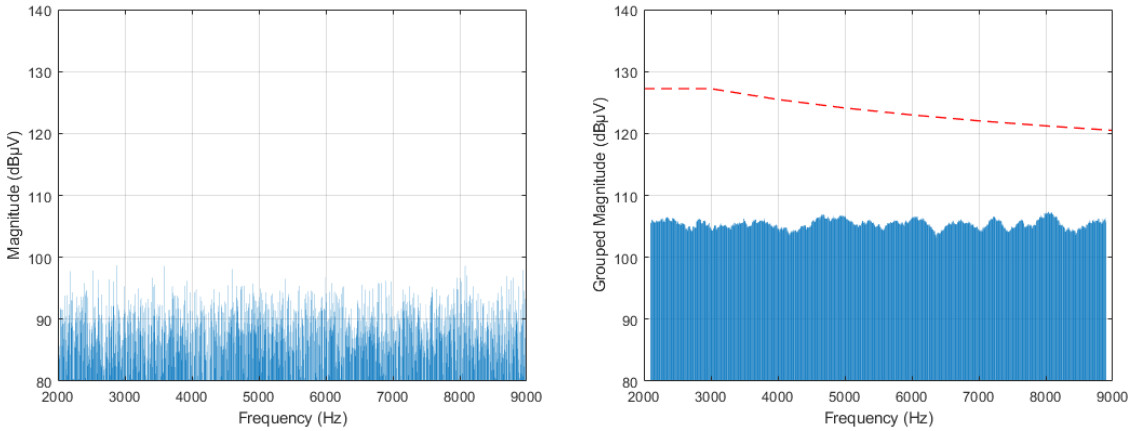

Figure 59: Drive B with loaded motor, voltage waveform in frequency domain (4.5 kHz, 510 rpm, 3.3 A)

Current waveforms in frequency domain are shown in Figure 60, indicating that at nominal output current and 510 rpm, the emissions are far from the limit. Surprisingly, the emissions have increased by approximately 10 dBµA, when compared to the measurements without a motor load in the EMC laboratory (Figure 42).

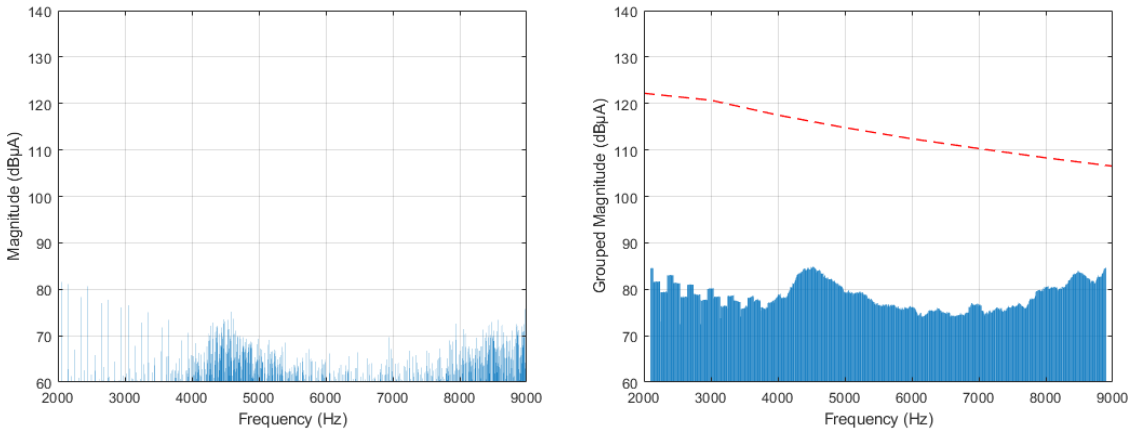

Figure 60: Drive B with loaded motor, current waveform in frequency domain (4.5 kHz, 510 rpm, 3.3 A)

The results from all measured operating points are presented in Appendix 2, showing the current emissions grouped in dBµA values. At 150 rpm speed, the peaks reach approximately 84 dBµA in all other load conditions except the lowest (1.0 A), where it is more consistent around 4.5 kHz. At 510 rpm, the peaks reach 85 dBµA, whereas at 1050 rpm they exceed 86 dBµA. Highest emissions are found in the lower end of the frequency range at 1500 rpm with nominal output current.

The emissions from all tested operating points remained well below the limit lines. The highest measured value around the switching frequency (4.5 kHz), is obtained in 1050 rpm speed with nominal output current, being approximately 86.2 dBµA. The lowest value near the 4.5 kHz frequency is measured at 150 rpm with 1.0 A (75.5 dBµA).

5.7 Conclusions for measurements

The measurement data from all test cases showed that the voltage and current harmonics remained below the limits specified in the IEC 61000-3-10 standard draft, with some cases indicating significantly low emission values in relation to the defined limits. With 4.5 kHz switching frequency, higher peaks were observed in the spectrum diagrams at 4.5 kHz and 9 kHz. With 1.5 kHz and 12 kHz switching frequencies, the emissions in the 2-9 kHz range were relatively consistent and low.

For Drive A, it was observed that having a longer motor cable resulted in a significant peak near 9 kHz frequency at 510 rpm. The deviation from the limit was only 2.9 dBµV and 3.1 dBµA. This indicates that if the emission limits stated in the draft remain unchanged, there may be challenges in the official compliance measurements in the future, when using long motor cables with this particular VSD model.

Drive B was tested with an unloaded motor using a 5 m long cable. The results showed low harmonic emissions in the 2-9 kHz range. When tested with a loaded motor, the current emissions increased by approximately 10 dBµA. However, due to the challenge of establishing a functional test setup in a laboratory with different infrastructure (e.g. longer cables, isolation transformer), the results were not directly comparable to the tests with an unloaded motor. Nevertheless, measured emissions remained far from the limit lines, with

some results being even 40 dBµA away from the limit. At the switching frequency of 4.5 kHz, the highest emissions were achieved at rated motor current and 1050 rpm (86.2 dBµA).

In the case of Drive C, the input-side IGBT rectifier caused having significant values around 6 kHz with a 5 m cable. The highest peaks were nearly 9 dBµA away from the limit. Drive C was also tested with a longer 100 m cable, which increased emissions by 5-10 dBµA at other frequencies, except for the prominent peak at 6 kHz where cable length had little impact. Based on the results, it is advisable to take into consideration the peak at 6 kHz in the possible product development of this drive, to ensure that emissions do not get worse.

Drive D was tested with and without an external AC-reactor, as the product structure does not contain an integrated choke in its DC-link. Even without the external AC-reactor, the emissions were low in relation to the limit line. With the AC-reactor installed, the emissions decreased by up to 15 dBµA in the middle frequency range.

The setup of the measurement equipment posed challenges and took a significant amount of time. The standard draft required to have frequency components at 5 Hz intervals. Despite the efforts, it was ultimately concluded that it was not possible to achieve data recording at 5 Hz intervals with WT5000 and ESW8, along with their connected sensors. The devices were only able to provide results at intervals of 50 Hz. This led to the issue with grouping of harmonics, as the grouping required calculations with components of 5 Hz intervals. As a result, the measurements were ultimately performed using an oscilloscope. In some cases, comparative measurements were conducted with the WT5000 and ESW8, and the results obtained were similar to those obtained with the oscilloscope.

The oscilloscope allowed for the easy measurement of voltage and current waveforms in the time domain. The challenge with the oscilloscope was to find the right measurement instruments to minimize interference. Additionally, MATLAB code had to be developed for further processing of the measurement data, which consumed a significant amount of time.

Despite the challenges in equipment usage, the WT5000 and ESW8 can provide sufficiently accurate measurements of harmonics in the range of 2-9 kHz for independent product evaluation purposes, even if the grouping is different from what is specified in the standard. However, official conformity testing would require software/firmware updates. It is expected that before IEC 61000-3-10 comes into effect, measurement equipment

manufacturers will offer updates to their products to provide user-friendly interfaces that facilitate the recording of harmonics in compliance with the new standard requirements.

6 Conclusions

This Master's thesis provided an overview of the upcoming IEC 61000-3-10 standard by examining the draft document prepared by IEC SC77A WG1. The main purpose of the standard is to define limits for disturbance voltage and current in the lower supra-harmonic frequency range (2-9 kHz) for electrical equipment having a rated line current up to 75 A.

During this work, harmonics of four different VSDs were measured in accordance with the IEC 61000-3-10 standard draft. Each VSD in this work was operating in the speed control mode, without loading the motor. Additionally, the smallest VSD was tested in the torque control mode with a loaded motor. In all test cases, the voltage and current harmonic emissions of the drives remained below the limit lines specified by the standard draft. Notably, when using a 150 m long motor cable for a VSD with 6-pulse rectifier, the emissions were elevated close to the limit at the higher end of the frequency range, as the system operated at 510 rpm.

During the measurements, the practical performance of the WT5000 power analyzer and the ESW8 EMI receiver in conducting measurements in accordance with the standard was investigated. Based on user experience, it was determined that the selected measurement instruments were unable to determine harmonics in accordance with the standard draft, as the instruments could not specify the grouping as required. However, despite this limitation, the instruments can provide sufficiently accurate measurements of harmonics in the 2-9 kHz range for independent product evaluation purposes.

During the work, the possibility of utilizing an existing VSD simulation model to assess harmonic emissions was also investigated. It was found that the simulation model was not accurate enough, thus making it unsuitable for compliance testing. Without the cable model, the simulated emissions were unrealistically low. However, when using a 150 m cable model, more realistic results were obtained, indicating the need to incorporate cable modeling in the further development of the simulation model. Appendix 3 displays the results previously illustrated in Figure 27 and Figure 38. It shows the comparison between the actual measurement results and simulation results for Drive A with a 150 m motor cable (operating point at 4.5 kHz / 510 rpm). In the simulation, there were high current harmonics at 5 kHz (almost 108 dBµA). In the actual measurements, the peaks were at 4.5 kHz and

were below 100 dBµA. Moreover, at the upper end of the frequency range, the simulated harmonics were approximately 14 dBµA lower than in the actual measurements.

The results of the study provided an overview of the supra-harmonic emissions in the 2-9 kHz range for the selected VSD models, as well as an overview of the suitability of the measurement equipment for these tests. Based on the experiences during this work, feedback can be provided to the IEC committee responsible for preparing the standard.

To gain more detailed insights, it would be beneficial to experiment with various motor cable lengths on different VSDs. Due to the low current rating of the AMN prototype, it was not used in testing of larger VSDs under load conditions. Therefore, it would be beneficial to develop a 75 A version of the AMN to accommodate for future extended testing with higher-power VSDs. This would allow for the evaluations of larger VSDs with heavily loaded motors and provide insights into their harmonic emissions.

References

ABB Drives, 2017. *Technical guide No. 6 - Guide to harmonics with AC drives.* ABB.

Arrillaga, J. & Watson, N. R., 2003. *Power system harmonics.* 2nd ed. ed. J. Wiley & Sons.

Csanyi, E., 2010. *Harmonic Distortion.* [Online]
Available at: https://electrical-engineering-portal.com/harmonic-distortion
[Accessed 2.4.2023].

Das, J., 2015. *Power system harmonics and passive filter designs.* 1st ed. John Wiley & Sons.

Davari, P., Hoene, E., Zare, F. & Blaabjerg, F., 2018. Improving 9-150 kHz EMI Performance of Single-Phase PFC Rectifier. *CIPS 2018; 10th International Conference on Integrated Power Electronics Systems.*

Erickson, R. W. & Maksimović, D., 2020. *Fundamentals of power electronics.* 3rd ed. ed. Springer.

Haapamäki, P. (2022) E-mail to Kari Ahlskog, 16 March.

IEC, 2009. *IEC 61000-4-7 Edition 2.1 - Testing and measurement techniques – General guide on harmonics and interharmonics measurements and instrumentation, for power supply systems and equipment connected thereto.* IEC.

IEC, 2017. *CISPR 16-1-2 Radio disturbance and immunity measuring apparatus – Coupling devices for conducted disturbance measurements.* IEC.

IEC, 2021. *IEC 61800-2 General requirements – Rating specifications for adjustable speed.* IEC.

IEC, 2022. *IEC 61800-3 EMC requirements and specific test methods for PDS and machine tools.* IEC.

IEC, 2023. *IEC 61000-3-10 Draft version G.* IEC.

Meyer, J. et al., 2018. Overview and Classification of Interferences in the Frequency Range 2-150 kHz (Supraharmonics). *2018 International Symposium on Power Electronics, Electrical Drives, Automation and Motion (SPEEDAM),* pp. 165-170.

Mohan, N., Robbins, W. P. & Undeland, T. M., 2003. *Power electronics : converters, applications, and design.* 3rd ed. ed. John Wiley & Sons.

Peeran, S. M. & Cascadden, C. W. P., 1995. Application, Design, and Specification of Harmonic Filters for Variable Frequency Drives. *IEEE TRANSACTIONS ON INDUSTRY APPLICATIONS,* 31(4).

Pinyol, R., 2015. *Harmonics: Causes, Effects and Minimization.* [Online]
Available at: https://www.salicru.com/files/pagina/72/278/jn004a01_whitepaper-armonics_(1).pdf
[Accessed 14.4.2023].

Rockwell Automation, 2014. *Application Guidelines for 12-Pulse Operation of PowerFlex 750-Series AC Drives.* [Online]
Available at: https://literature.rockwellautomation.com/idc/groups/literature/documents/at/750-at003_-en-p.pdf
[Accessed 25.4.2023].

Schwarzbeck - Mess-Elektronik, 2023. *NNLK 8121 - Line Impedance Stabilisation Network.* [Online]
Available at: https://www.schwarzbeck.de/en/lisn-line-impedance-stabilisation-networks/v-lisn-en/v-lisn-cispr-16-1-2/304-nnlk-8121.html
[Accessed 10.4.2023].

Stevanović, I., Wunsch, B., Madonna, G. & Skibin, S., 2014. High-Frequency Behavioral Multiconductor Cable Modeling for EMI Simulations in Power Electronics. *IEEE Transactions On Industrial Informatics,* 10(2), pp. 1392-1400.

Tektronix, 2012. *MDO4000 Series - Mixed Domain Oscilloscopes - User Manual.* [Online]
Available at: https://www.tek.com/en/oscilloscope/mdo4000-mixed-domain-oscilloscope-manual/mdo4000-series-0
[Accessed 5.7.2023].

Appendix 1. Tested variable speed drives

VSD name	Nominal power	Main features	Motor & Cable
Drive A	37 kW	6-p diode rectifier, Internal DC Choke	37 kW, 1475 rpm 16 mm^2 MCCMK (5 m & 150 m)
Drive B	1.1 kW	6-p diode rectifier, Internal DC Choke	1.5 kW, 1420 rpm 2.5 mm^2 MCCMK (5 m)
Drive C	37 kW	IGBT rectifier (AFE drive), LCL filter	37 kW, 1475 rpm 16 mm^2 MCCMK (5 m & 100 m)
Drive D	22 kW	6-p diode rectifier, External AC Choke	22 kW, 1474 rpm 25 mm^2 MCCMK (10 m)

Appendix 2. Drive B measurements with load

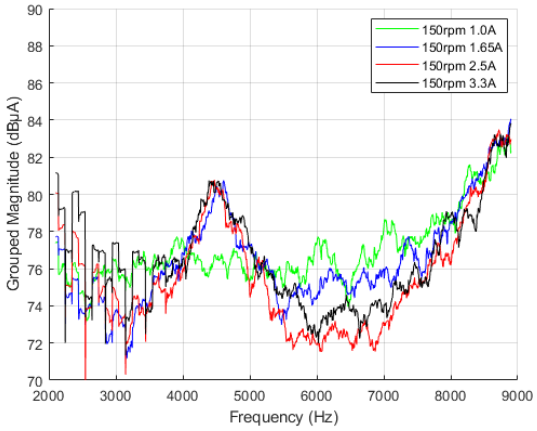

150 rpm

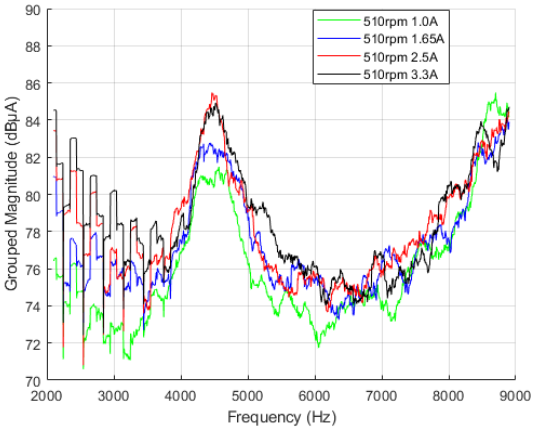

510 rpm

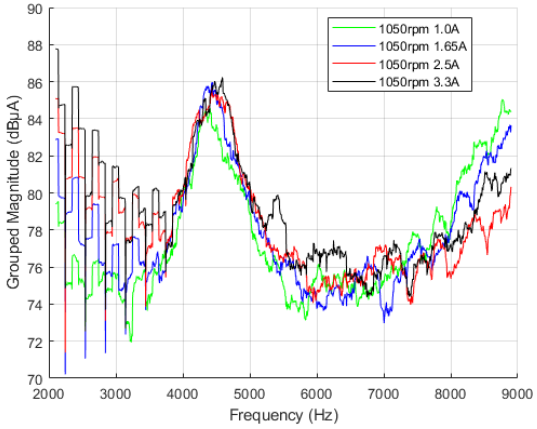

1050 rpm

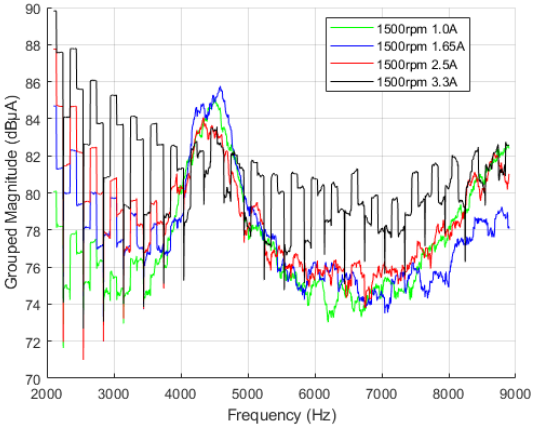

1500 rpm

Appendix 3. Current harmonics of Drive A with 150 m motor cable, simulation vs actual measurement comparison

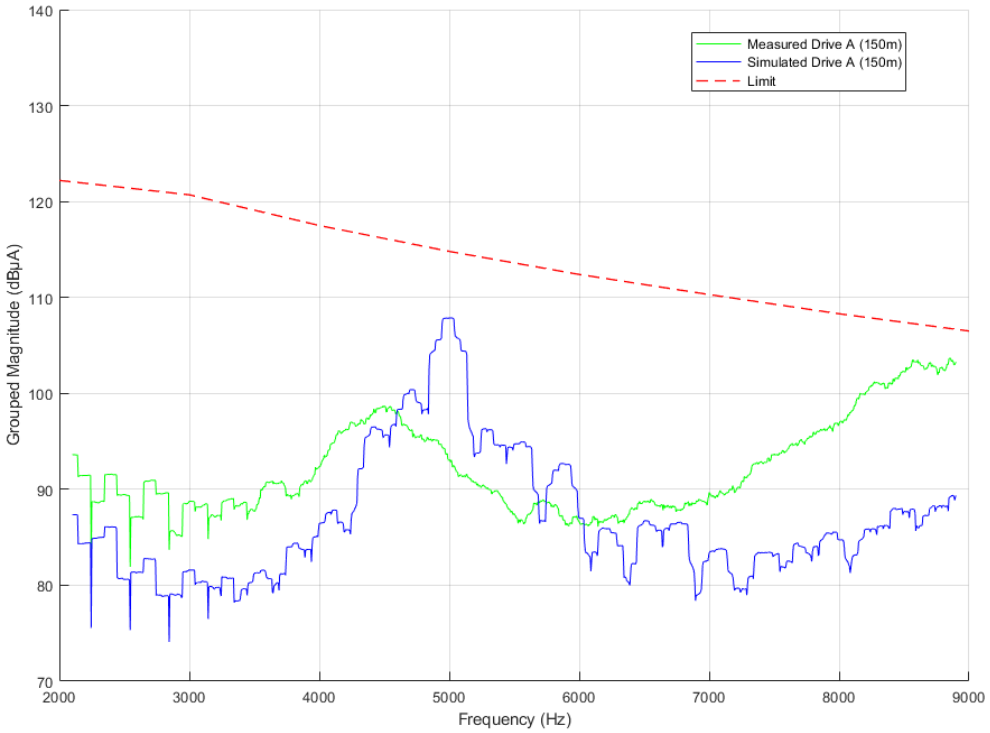

The switching frequency was 4.5 kHz. The motor speed was 510 rpm. No load was put on the motor.